Forest Ecology and Management 526 (2022) 120582

Contents lists available at ScienceDirect

Forest Ecology and Management

journal homepage: www.elsevier.com/locate/foreco

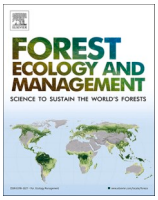

Intermediate-severity disturbance impacts in a mixedwood forest: A multi-scale analysis

J. Davis Goode [a,*], Anuska Narayanan [a], David L. Phillips [a], Justin L. Hart [a], Scott J. Torreano [b], Daniel C. Dey [c]

[a] Department of Geography, University of Alabama, Box 870322, Tuscaloosa, AL 35487, USA
[b] Department of Earth and Environmental Systems, University of the South, 735 University Ave., Sewanee, TN 37383, USA
[c] USDA Forest Service, Northern Research Station, Columbia, MO 65211, USA

ARTICLE INFO

Keywords:
Shortleaf pine
Oak-pine
Remote sensing
Tree survival
Tree mortality
Spatial patterns
Canopy openings
Natural disturbance-based silviculture

ABSTRACT

Mixed *Quercus-Pinus* stands are increasingly desired by forest managers to achieve a range of objectives, including biodiversity enhancement and resilience to global change. To create and perpetuate desired mixed *Quercus-Pinus* stand composition and structure, quantitative information on natural disturbance impacts on stand development and succession is necessary. Wind is the most common natural canopy disturbance in eastern North America, and impacts vary in severity and spatiotemporal scales. Intermediate-severity disturbance (ISD; events that occur along a classification gradient between frequent gap-scale and infrequent, stand-replacing events) is hypothesized to be an important driver of mixed *Quercus-Pinus* creation and maintenance. Our overarching goal was to quantify patterns of intermediate-severity wind disturbance in a mixed *Quercus-Pinus echinata* Mill. forest on the Cumberland Plateau in Tennessee, USA. Specifically, our objectives were to: 1) quantify post-disturbance species composition, stand structure, and residual tree spatial patterns, 2) infer individual-tree, neighborhood, and site-specific impacts on tree mortality, and 3) describe frequency, size, shape, and spatial distribution of ISD-created canopy openings. We inventoried plots in *Pinus echinata*-dominated, disturbance-impacted portions of the forest. To infer individual-tree and spatially-explicit neighborhood characteristics that influenced survival probability, we applied a random forest classification algorithm. To document changes in tree spatial distribution before and after disturbance, we used spatial point pattern analysis. To characterize forest-scale disturbance patterns, we classified canopy gaps from high-resolution orthoimagery. The most important predictors of survival were basal area, taxonomic group, and distance to nearest neighbor. Pre-disturbance trees and residuals were spatially randomly distributed. Most detected openings were 50–150 m^2, and the opening size-frequency distribution exhibited a reverse J-shape. Openings were spatially clustered within the forest at distances < 200 m and complex in shape. We provide quantitative recommendations on the frequency, size, shape, and spatial distribution of silvicultural entries patterned after natural disturbance. To emulate natural disturbance patterns, we recommend patch seedtree harvests with reserves or patch clearcuts with reserves, and these harvest-created openings should be concentrated (i.e., clustered) in portions of the stand in which *P. echinata* is most dominant and/or most competitive. Site preparation with prescribed fire, herbicide, and/or mechanical thinning may also be necessary to prepare the seedbed and reduce hardwood competition to favor *Pinus* establishment in openings.

1. Introduction

Forest disturbances alter the species composition, stand structure, and ecosystem function of forests globally (Foster et al., 1998; White and Jentsch, 2001; Seidl et al. 2017). All forests experience disturbance and are in a constant state of recovery. Forest disturbances are typically classified based on severity, spatial extent, seasonality, and frequency; and range from frequent, small events to infrequent, large, stand-replacing events (Oliver and Larson 1996). Intermediate-severity disturbances (ISD) are those that occur between each endpoint of the disturbance severity gradient (Hart and Kleinman 2018). Although relatively understudied compared to gap-scale and stand-replacing disturbances, ISD may be a more influential driver of forest ecosystem change than is typically understood (Hart and Kleinman 2018, Meigs

* Corresponding author.
E-mail address: jdgoode2@crimson.ua.edu (J. Davis Goode).

https://doi.org/10.1016/j.foreco.2022.120582
Received 14 June 2022; Received in revised form 27 September 2022; Accepted 5 October 2022
Available online 19 October 2022

and Keeton 2018; Nagel et al., 2021), as these events typically have a shorter return interval than the lifespan of most canopy trees (Seymour et al., 2002; Hart et al., 2012; Cowden et al., 2014; Hart and Cox 2017), and they provide opportunity for a diversity of tree reproduction to establish and ascend into the overstory. At the stand level, ISD may result in a high frequency of localized events, a single large opening, or some combination of canopy openings across a wide range of sizes (Canham et al., 2001; Woods 2004; Nagel and Svoboda 2008). Canopy openings may be clustered, dispersed, or randomly distributed across stands, forests, and landscapes (Frelich and Reich 1995; Habashi 2019; Paluch and Jastrzębski, 2022). Intermediate-severity disturbance agents may include insect and pest outbreaks (e.g. Axelson et al., 2010), ice storms (e.g. Covey et al., 2015), wind storms (e.g. Cowden et al., 2014), and fires (e.g. Fulé et al., 2003). Among these canopy disturbance agents, wind is the most common in forests of eastern North America (Runkle 1985; Peterson et al. 2016).

Wind disturbance severity is influenced by multiple interacting factors that include storm characteristics, topography, and species composition and stand structure. Atmospheric disturbances may produce strong winds associated with downbursts and tornados generated by convective systems, hurricanes, and topographically induced downslope winds (Hjelmfelt et al., 2010). Intermediate-severity wind disturbance has been studied following low-intensity tornados (e.g. < EF 2; Cox et al., 2016), hurricanes (Busing et al., 2008), derechos (Daniels et al., 2020), and downbursts (Battles et al., 2017). Individual-tree susceptibility to wind disturbance is influenced by individual-tree characteristics, neighborhood effects, and site conditions, but tree diameter is often the most consistent predictor of wind-induced mortality (Peterson 2007). Large-diameter trees, trees with low wood density, and those with shallow rooting depth are more susceptible to snapping and uprooting in wind disturbances (Salas-Eljatib and Weiskittel 2020). Neighborhood effects such as distance to nearest neighbor and neighborhood composition (Frelich, 2016; Rutledge et al., 2021), and site characteristics such as soil properties, topography, and underlying geology may also influence tree mortality patterns (Waldron et al., 2013).

Intermediate-severity wind disturbance often results in irregular patterns of severity across space and a diverse arrangement of biological legacies (Meigs and Keeton 2018). Therefore, heterogenous spatial patterns of canopy openings, post-disturbance forest structure, initial floristics and other biological legacies may favor the establishment and recruitment of woody plant species with a variety of life-history strategies and functional traits. Intermediate-severity wind disturbance combined with recurring low-intensity fire may be required to maintain certain species assemblages. An example is mixed *Quercus-Pinus* systems of the eastern United States, in which wind disturbance is the most common canopy disturbance agent (Peterson et al., 2016). Mixed *Quercus-Pinus* ecosystems span millions of hectares in this region, but this forest type has experienced a dramatic decrease in extent (Oswalt et al., 2012). *Quercus-Pinus* stands exists in a mid-successional state (Cooper 1989). In this successional pathway, dominance of the faster growing, shade-intolerant *Pinus* spp. transitions to the more shade-tolerant *Quercus* spp. in the absence of the appropriate combination of fire and canopy disturbance. Land-use change, altered disturbance regimes, the proliferation of commercial *Pinus* plantations, and lack of active management have dramatically reduced the extent of mixed *Quercus-Pinus* forests (Oswalt et al., 2012, Vickers et al. 2021). Mixed *Quercus-Pinus echinata* stands of the eastern USA serve as an excellent model to investigate patterns of canopy disturbance, succession, and development to enhance the inherently complex management of these ecosystems, which often emphasizes accelerating or reversing succession through manipulating the disturbance regime. Because of the wide ecological amplitude of *Pinus echinata*, it is well suited to co-occur with a variety of hardwood species under certain disturbance regimes (Lawson and Kitchens 1983).

To create and perpetuate mixed *Quercus-Pinus echinata* stands, it is critical to evaluate the multi-scale impacts of canopy disturbance on species composition and stand structure. Therefore, our overarching goal was to quantify impacts of intermediate-severity wind disturbance in a mixed *Quercus-Pinus echinata* forest on the Cumberland Plateau in Tennessee, USA. Specifically, our objectives were to: 1) quantify post-disturbance species composition, stand structure, and residual tree spatial patterns, 2) infer individual-tree, neighborhood, and site-specific impacts on tree mortality, and 3) describe frequency, size, and spatial distribution of ISD-created canopy openings. Although individual-tree susceptibility to mortality has been well studied (Peterson et al. 2016), mortality may be confounded by interactions of disturbance agents contributing to mortality, neighborhood characteristics, site conditions, and species-specific traits. A comprehensive understanding of individual-tree susceptibility may inform the design of silvicultural systems that limit economic loss during and after wind disturbance while also maintaining desired species composition and structure. Furthermore, quantitative information on size, shape, frequency, and spatial pattern of canopy openings is essential to design silvicultural entries commensurate with natural patterns of disturbance and development. Our results inform mixedwood silvicultural systems and enhance our understanding of the necessary disturbance regime to create and perpetuate resilient, biodiverse, and structurally complex mixed *Quercus-Pinus echinata* ecosystems.

2. Methods

2.1. Study site

Our study occurred in a wind-disturbed mixed *Quercus-Pinus echinata* forest of Savage Gulf Natural Area (SGNA) in Tennessee, USA. The SGNA is a 6,309 ha state natural area managed by the Tennessee Department of Environment and Conservation. Because of its biodiversity and unique geological characteristics, the reserve is listed as a National Natural Landmark by the US Department of the Interior. See Hart et al. (2012) for a detailed description of settlement history, prior land use, species composition and structure, and canopy disturbance history. The SGNA is located on the Cumberland Plateau section of the Appalachian Plateaus physiographic province, the westernmost physiographic province of the Appalachian Highland realm (Fenneman 1938). The Cumberland Plateau section is characterized by broad, uncut plateau remnants not yet maturely dissected that are situated between deep valleys (Fenneman 1938). In this study, disturbance sampling plots were established on the weakly dissected plateau landtype association of the true plateau subregion as classified by Smalley (1986), characterized by broad undulating to rolling ridges with gentle to moderately steep-sided slopes, dissected by young valleys. The tablelands above Savage Creek, a deeply incised tributary to the Collins River, are dissected by bedrock streams. The underlying geology of the SGNA is in the Crab Orchard and Crooked Forked groups, which are primarily composed of sandstone, conglomerate, siltstone, shale, and coal. Soil Series of the study area are Beersheba, Jefferson, Lily, Lonewood, and Ramsey (USDA NRCS 2022), which are characterized as being moderately to very deep and well drained. These Soil Series are primarily derived from sandstone, shale, siltstone, or quartzite, with loam, silt loam, and sandy loam textures (USDA NRCS 2022). The regional climate of the SGNA is humid mesothermal (Thornthwaite 1948), with long, moderately hot summers and short, mild winters. Mean annual temperature is 13.3° C, with the lowest monthly mean temperature of 2.3° C in January and the highest monthly mean temperature of 23.4° C in July (PRISM 2022). The amount of precipitation is typically steady throughout the year with a mean annual total of 1,607.3 mm. October receives the lowest mean precipitation (91.9 mm) and March receives the greatest mean precipitation (154.9 mm, PRISM 2022).

The Cumberland Plateau supports diverse plant communities that are intermediate between mixed mesophytic, mixed hardwood, and mixed *Pinus*-hardwood forest types (Hinkle 1978, 1989). On upland sites

of the Cumberland Plateau, including the tablelands of the SGNA, plant community composition is a function of fine-scale topographic characteristics, soil water availability, and canopy disturbance history (Hinkle 1978, Smalley 1986, Hart et al. 2012). The contemporary woody plant assemblage of the SGNA tablelands is dominated by *Quercus alba*, *Acer rubrum*, and *P. echinata* (Hart et al. 2012). At the genus level, *Quercus* is the most dominant (46 % basal area), followed by *Pinus* (17 % basal area), and *Acer* (16 % basal area). *Quercus* spp. and *Pinus* spp. represent 70 % of canopy trees, and *Oxydendrum arboreum* and *Acer rubrum* represent the majority of understory trees (Hart et al. 2012). Interestingly, these taxa represent a wide range of silvical characteristics. For example, shade tolerance varies widely from the shade intolerant *P. echinata* to the shade tolerant *A. rubrum*. *Pinus echinata* occurs in spatially clustered neighborhoods in what is an otherwise *Quercus* dominated forest (Goode et al., 2021).

The most frequent contemporary natural disturbance agent in the SGNA is wind, with 103 recorded wind-related storm events from 1950 to 2019 that caused significant tree or structural damage (NOAA Storm Events Database 2022). The return interval for ISD events in the SGNA is ca. 50 years (Hart et al. 2012) and the last detected ISD event in this forest occurred in 1976 (Goode et al. 2021). A reconstruction of fire history revealed that mean fire interval for SGNA between 1834 and 1935 was 2.5 years, and increased to 13.7 years after 1940 during an extended period of fire exclusion (Stambaugh et al. 2020).

On 6 November 2018, a quasi-linear convective system with imbedded tornados impacted portions of central Tennessee. The systems produced ten tornados, and among those, one EF-1 tornado dissipated immediately prior to reaching SGNA. Although official storm surveys indicated that the tornado did not impact SGNA, the same storm system produced microburst wind damage that uprooted and snapped many canopy stems on the eastern tablelands of SGNA (NOAA Storm Events Database 2022). This wind event offered an excellent opportunity to examine the impacts of intermediate-severity disturbance at the individual-tree and stand-scales in a mixed *Quercus-Pinus echinata* forest. We were specifically interested in the impacts of this disturbance in *P. echinata* dominated neighborhoods, by evaluating post-disturbance successional trajectories and quantifying *P. echinata* patch resilience.

2.2. Field methods

To quantify impacts of wind disturbance on *P. echinata*-dominated neighborhoods, we established 0.04 ha fixed-radius plots using predetermined criteria. To be considered for use, a plot must have: (1) been directly impacted by the wind event, (2) contained at least four canopy *P. echinata* stems (≥30 cm diameter at breast height, dbh; residual or senesced), and (3) contained at least four pieces of coarse woody debris (CWD ≥ 10 cm diameter; to include the aforementioned *P. echinata*). We walked a predetermined transect within SGNA until we encountered an area that met our criteria. After establishing and sampling a plot in this area, we then walked a new transect based on a new, random azimuth and sampled any plots along this azimuth that satisfied our criteria. Once no new plots were encountered along this new azimuth, we returned to and continued along our predetermined transect. Using this method, we sampled 32 plots (1.28 ha).

To determine plot composition and structure, we sampled trees (live woody stems ≥ 5 cm dbh), saplings (live woody stems < 5 cm dbh, ≥ 1 m height), seedlings (live woody stems < 1 m height), and CWD and standing dead trees (dead woody stems ≥ 10 cm dbh). For each tree, we recorded species, dbh, and crown class (based on the amount of intercepted light; overtopped, intermediate, co-dominant, and dominant; Oliver and Larson 1996). For saplings, we recorded species and tallied abundance. We sampled seedlings in a nested 0.002 ha subplot (20 m^2) located at plot center, and recorded seedling species and abundance. Coarse woody debris was assigned a decay class (1–5; based on Forest Inventory and Analysis program; FIA 2005) and classified as either standing or downed. Standing CWD was further classified as snags (crown mostly intact) or snaps (crown removed), identified to species, and measured for dbh. Downed CWD was further classified as uproots (root plate intact) or logs (root plate removed; ≥ 1.3 m in length), identified to species, and measured for length (excluding portions outside the plot boundary). Uproots were measured for dbh 1.37 m above the attached root plate, and logs were measured for diameter at both ends or where the log intersected the plot boundary.

At each plot, we recorded the latitude and longitude of plot center using a Trimble Juno t41/5 GPS receiver. We used hemispherical photographs taken 1 m above the ground at plot center to quantify canopy openness. Photographs were captured using an Olympus Stylus TG-3 digital camera mounted on a self-leveling tripod, fitted with a 180° field of view fisheye lens, and calibrated for use with WinSCANOPY software (WinSCANOPY, Regent Instruments, Quebec City, Quebec, Canada). To analyze spatial patterns, we recorded the distance and azimuth from plot center to each tree and CWD. For CWD, distance and azimuth were recorded for both ends of the CWD, or where the CWD intersected the plot boundary. To determine the age of canopy *P. echinata* stems, we used an increment borer to extract a tree-ring sample from the largest diameter *P. echinata* within or directly adjacent to the plot.

2.3. Analytical methods

2.3.1. Species composition, stand structure, and disturbance severity

To quantify disturbance severity variability and infer the drivers of mortality for analyses described below, we calculated multiple biotic and abiotic disturbance response and explanatory variables. Response variables included canopy openness, standing CWD basal area (snags and snapped stems, m^2 $plot^{-1}$), downed CWD volume (logs and uproots, m^3 $plot^{-1}$), and Shannon Damage Heterogeneity Index (Peterson 2019). To remove background mortality from canopy disturbance unrelated to the ISD, we calculated all CWD metrics for decay class I and II individuals only. Explanatory variables included mean age of canopy *P. echinita*, transformed aspect (Beers et al. 1966), slope, pre-disturbance tree Shannon diversity (with CWD considered), and relative *Pinus* basal area $plot^{-1}$.

Canopy openness (%) was quantified using the software WinSCANOPY. Shannon Damage Heterogeneity Index (Sh-DHI, Peterson 2019) was used to quantify post-disturbance structural complexity based on the diversity in composition and mode of death of CWD. For this metric, we considered CWD species + MOD as individual "species," and calculated Sh-DHI for each plot. To calculate volume of logs, we used the equation for a conic paraboloid (Fraver et al., 2007). To calculate volume for uprooted stems, species-specific allometric equations were used (Woodall et al., 2011; Parker and Hart, 2014). To determine the average age of canopy *P. echininata*, extracted tree-ring samples were processed based on the methods outlined in Stokes and Smiley (1996). Samples were air dried, mounted with cells vertically aligned, and sanded to reveal cellular structure. Tree rings were then dated to the calendar year of formation with the aid of a stereozoom macroscope. Pith estimators were used to estimate tree age based on visible ring curvature when samples lacked pith (Villalba and Veblen, 1997).

To quantify the composition and structure of residual trees, saplings, and seedlings, we calculated standard descriptors, species richness, and Shannon diversity. For trees, standard descriptors included density (stems ha^{-1}), relative density (contribution to total tree density), dominance (basal area, m^2ha^{-1}), relative dominance (contribution to total basal area), and importance (mean of relative dominance and density).

2.3.2. Classification of survival probability

Traditionally, logistic regression is used to model tree mortality. However, logistic regression is sensitive to class imbalance (i.e., more live trees than dead trees). Therefore, to infer the drivers of individual-tree mortality, we applied a random forest machine-learning

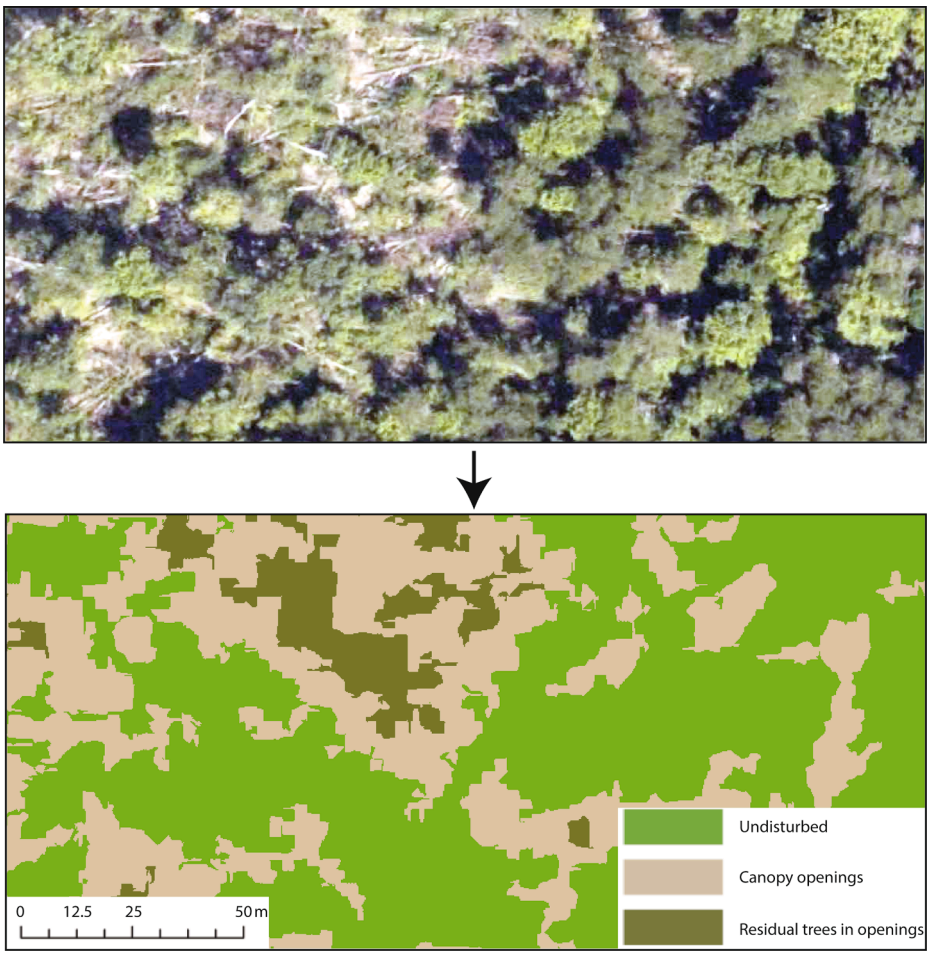

Fig. 1. Fine-scale example of pixel-based classification scheme to classify canopy openings from true-color orthoimagery captured after a November 2018 intermediate-severity wind disturbance in Savage Gulf State Natural Area, TN, USA. User-defined training samples were created for shadows, bare ground, and forest and classified into three categories: undisturbed forest, canopy openings, residual trees in openings using a support vector machine learning algorithm.

classification algorithm with balanced classes, which has been shown to be more robust to problems with imbalanced data (Shearman et al. 2019). Random forest is an adaptation of classification and regression trees, in which each tree casts a vote for each class (alive vs dead) based on randomly sampled predictor variables (Liaw and Wiener 2002). For each classification tree, a random set of samples and predictor variables is selected with replacement, and those not selected are termed "out-of-bag" (OOB) and utilized to evaluate error. However, when classes are severely imbalanced, the likelihood of selecting the minority class in the bootstrapped sample is low. Chen et al. (2004) proposed a balanced random forest algorithm, in which an equal number of observations from each class is sampled at each tree. We used the "randomforest" package in R to determine the individual and plot-level predictors that influenced individual-tree survival from a sample of 415 live trees and 114 dead trees $\geq$ 15 cm dbh.

Individual-tree predictor variables included taxonomic group, basal area ($m^2 tree^{-1}$), distance to nearest neighbor (m), taxonomic group of nearest neighbor, and dominance. Dominance is a spatially-explicit competition metric that quantifies the diameter differentiation of a five tree neighborhood (Aguirre et al. 2003). Dominance is the proportion of the four nearest neighbors that are of a smaller diameter than the focal tree, and assumes five values from 0 to 1. To reduce edge bias in the calculation of dominance, the NN1 edge correction was applied. (Pommerening and Stoyan 2006). Aggregated plot-level predictors included Shannon diversity, relative *Pinus* basal area (percent contribution to total plot basal area), mean age of trees within or in proximity to the plot, and the Clark and Evans index. The Clark and Evans index (Clark and Evans 1954) is a crude measure of aggregation of a point pattern, with values > 1 indicating random pattern and values < 1 indicating clustered pattern.

We randomly selected 70 % of the data to train the model and withheld 30 % of the data for model validation (testing). We set the *sampsize* parameter to select the maximum number of dead trees from the training dataset (n = 85) for each classification tree (i.e., 85 trees from the live and dead classes were selected). The final model was hyper-tuned to optimize the number of trees grown at each split (*ntree* = 500) and number of variables chosen at each split (*mtry* = 3). These parameters were selected after fitting multiple models and selecting the model with the lowest OOB error and the greatest predictive performance. Model performance was evaluated by plotting the receiver operating characteristic curve, and subsequently calculating the area under the curve (AUC). The AUC provides an indication of the predictive ability of the model, with greater AUC values indicating enhanced differentiation in classification between live and dead trees (Hosmer and Lemesbow, 1980). Final model accuracy was determined by predicting survival of trees in the training dataset and calculating classification sensitivity and specificity. Sensitivity is the percentage of true positives (live trees) and specificity is the percentage of true negatives (dead trees). To determine the relative importance of predictor variables in the final model, we calculated mean decrease Gini, which quantifies the total decrease in node impurity averaged over all classification trees (Wang et al. 2016). Greater mean decrease Gini values for a given predictor indicate greater importance. We created partial dependence plots to visualize how probability of survival was influenced by variability in

predictor variables over their distribution (e.g. visualize how probability of survival was influence by variability in tree basal area) when all other predictors are held constant. We constructed partial dependence plots for the three most important predictor variables (as determined by mean decrease Gini) with the package "pdp" in R (Greenwell 2017).

2.3.3. Canopy gap detection

To identify disturbance-created canopy openings at the forest scale, we performed a pixel-based image classification on high-resolution orthoimagery. We selected a 174 ha portion of SGNA that was of mature mixed *Quercus-Pinus echinata* composition and structure and was directly impacted by the 2018 wind event. Vexcel Imaging "Blue Sky" imagery (Vexcel Imaging 2022) was acquired from the Tennessee State government's aerial imagery program. Images of the study site were captured 10 months after the disturbance event, between 18 and 28 August 2019 with a Condor M1 4-band sensor mounted to a fixed wing aircraft (Vexcel Imaging 2022). These images were collected with a ground sampling distance of 20 cm and a horizontal and vertical accuracy of 120 cm. All image post-processing (geometric and atmospheric corrections) was performed with the software UltraMap TE (Vexcel Imaging 2022) prior to retrieving the data.

Image classification was conducted in ArcGIS Pro (ESRI 2022). To identify canopy openings, we used supervised, pixel-based classification of the true-color raster image. Support vector machine (SVM) learning was used classify the image based on user-defined training samples. SVM is a non-parametric classifier that is robust to pixel complexity in raster images (Tzotsos & Argialas, 2008), does not require a large number of training samples, and has been shown to classify images with a higher accuracy compared to other classification algorithms (Lawrence 2022). A training class schema was created with three classes based on the true-color raster: shadow (n = 150), barren (n = 150), and forest (n = 150). Shadows indicate a break in continuous canopy cover in which the canopy trees on the edge of the openings cast shadows into the openings. During image capture in August 2019 at 35.45° N and 85.62° W, the declination of the sun was ca. 13° N (NOAA Solar Position Calculator 2022). Therefore, we were confident that shadows were evidence of canopy openings at date of image capture.

The Image Classification Wizard in ArcGIS Pro was used to classify the raster image (Fig. 1). We selected supervised, pixel-based classification, with the classification schema of three classes (shadow, barren, forest) and 450 training samples (150 class^{-1}), SVM as the classification algorithm, and the true-color raster as the image to be classified. We created a final stand-cover map with two classes: canopy openings (shadow + barren) and forest. Openings were classified as contiguous pixels classified as openings and > 50 m^2, which is the most frequent minimum gap size found in the literature (e.g Hart and Kupfer 2011). We used a 200 m^2 threshold to distinguish between large openings and small openings (single or multi-tree gaps, Hobi et al. 2015, Richards and Hart 2011, Sefidi et al. 2011, Yamamoto 1995). We identified residual trees in openings as pixels > 6 m^2 classified as forests and completely contained within pixels classified as openings. Accuracy assessment was conducted on the final classified image with the Accuracy Assessment tool in ArcGIS Pro. A stratified random sampling approach was used, with 100 points randomly distributed within each of the three classes. For each of the 300 points, the true-color image was used to determine if the point was located in shadow, barren, or forest class by an unbiased user. These data were compared to the classified image and a confusion matrix was produced to assess overall accuracy, user accuracy, producer accuracy, and the Kappa Index.

To quantify the frequency, size, and shape irregularity of detected canopy openings, we used the package "landscapemetrics" in R (Hesselbarth et al. 2019). This package is an adaptation of the commonly used FragStats landscape metrics toolbox (McGarigal et al. 2012). For all openings, small openings ($<$200 m^2), and large openings ($\geq$200 m^2), we calculated landscape metrics to characterize opening heterogeneity across the forest. The metrics calculated for each class included: 1) number of openings, 2) mean area of openings, 3) mean perimeter of openings, 4) mean perimeter to area ratio, 5) mean shape complexity, and 6) mean distance to nearest opening. The shape complexity index (FRAC) increases with increased opening shape complexity, with values from 1 (perfect square) to 2 (irregular polygon).

2.3.4. Spatial analyses of trees and canopy openings

To determine disturbance-induced change in horizontal tree spatial patterns, we considered snag, snapped, and uproot locations combined with residual tree locations to reconstruct pre-disturbance tree spatial patterns. Because sampling plots were disjunct in space and circular in shape, we truncated and adjoined sampling plots to create a contiguous 4 × 8 grid of 16 × 16 m square plots (Woodall and Graham 2004). Individual plot-level spatial point pattern analysis was not feasible because multiple plots had fewer than four residual trees, which would preclude meaningful results. We determined the maximum size of a square that occurs completely within the circular sampling plot and excluded all trees and CWD that occurred between the boundary of the square plot and the border of the circular plot. The location of each square plot was randomized and placed into a 4 × 8 m contiguous grid.

We used a spatial point pattern approach to quantify spatial patterns of reconstructed pre-disturbance trees and post-disturbance residuals to determine if trees or residuals were clustered, random, or dispersed in horizontal space. We used the pair correlation function *g(r)* individually on both pre-disturbance and post-disturbance trees. This function is a second-order, non-cumulative modification of the commonly used Ripley's K function (Stoyan and Stoyan 1996). The *g(r)* quantifies the number of points within annuli at multiple distances *(r)* relative to expected randomly distributed points (Baddeley et al., 2015). To test for significant spatial clustering or dispersion, we contrasted observed data to the upper and lower bounds of confidence envelopes. The 95 % confidence envelopes were constructed from 99 Monte Carlo simulations under the assumption of complete spatial randomness. The univariate spatial pattern was defined as clumped, random, or dispersed if the pattern was above, within, or below the confidence envelope, respectively, at distance *(d)*. A goodness-of-fit test for the null hypothesis was also performed. The *g(r)* was performed at a 1 m lag distance and did not exceed half the minimum length of the grid (32 m). To account for edge effects, an isotropic edge correction was applied. Univariate point pattern analyses were performed with the package "spatstat" in R (Baddeley and Turner, 2005). Because individual plots were truncated and combined (Woodall and Graham 2004), results from this point pattern analysis approach should be interpreted with caution as the method used here is not as robust as if it were applied to a large contiguous plot (Gray et al. 2018).

To quantify the spatial distribution of detected canopy openings, we used a modified point pattern analysis approach for objects with finite size and real shape with the grid-based software Programita (Wiegand and Moloney, 2014). We reclassified the stand-cover raster from 0.2 m pixel size to 5 m pixels for spatial analyses. If the pixel directly adjacent to a gap pixel was also classified as gap, the software grouped these pixels as one contiguous canopy opening. This process was crucial for grouping pixels as one opening unit for the randomized simulation procedure. To avoid the biases introduced from the cumulative nature of Ripley's K, we used the non-cumulative O-ring statistic to quantify the patterns of openings. We quantified the spatial patterns of all openings, small openings ($<$200 m^2), and large openings ($\geq$200 m^2). We compared the spatial patterns of detected openings to confidence envelopes simulated 99 times under the assumption of complete spatial randomness.

Table 1
Basal area (standing snags and snapped stems; m^2ha^{-1}), relative basal area (%), volume (downed logs and uproots; m^3ha^{-1}), and relative volume (%) for all coarse woody debris > 10 cm diameter in a wind-disturbed forest at Savage Gulf State Natural Area, TN, USA. Species are ranked by relative basal area.

	Basal area (m^2ha^1)	Relative basal area (%)	Volume (m^3ha^1)	Relative volume (%)
Pinus virginiana Mill.	1.96	38.4	24.63	23.7
Quercus coccinea Münchh.	1.30	25.5	25.58	24.7
Quercus alba L.	0.69	13.6	5.17	5.0
Pinus echinata Mill.	0.47	9.2	16.09	15.5
Quercus rubra L.	0.35	6.8	15.90	15.3
Quercus spp.	0.12	2.4	0.30	0.3
Oxydendrum arboreum (L.) DC.	0.07	1.3	1.36	1.3
Liriodendron tulipifera L.	0.06	1.2	0.06	0.1
Nyssa sylvatica Marshall	0.05	0.9	0.44	0.4
Carya tomentosa L.	0.02	0.4	0.21	0.2
Acer rubrum L.	0.01	0.2	1.09	1.0
Pinus spp.	0.00	0.0	8.69	8.4
Quercus velutina Lam.	0.00	0.0	2.16	2.1
Diospyros virginiana L.	0.00	0.0	1.21	1.2
Hardwood spp.	0.00	0.0	0.83	0.8
Sassafras albidum (Nutt.) Nees	0.00	0.0	0.02	0.0
TOTALS	**5.11**	**100.0**	**103.73**	**100.0**

3. Results

3.1. Composition, structure, and spatial patterns of woody plant survival and mortality

We documented 5.11 m^2/ha of standing CWD and 103.73 m^3 ha^{-1} of downed decay class I and II CWD (Table 1). Plot-level impacts were variable, ranging from 0.98 m^2 $plot^{-1}$ (19.67 m^2/ha) standing CWD to no standing CWD. Downed CWD volume was similarly variable across plots, ranging from 11.18 m^3 $plot^{-1}$ (155.20 m^3 ha^{-1}) to 0.75 m^3 $plot^{-1}$ (23.00 m^3 ha^{-1}). Mean Sh–DDI was 1.51 ± 0.08 (SE), with a plot-level range of 2.41–0.63. At the species level, *Pinus virginiana* had most basal area lost (1.96 m^2/ha standing CWD), followed by *Q. coccinea* (1.30 m^2/ha) and *Q. alba* (Table 1; 0.69 m^2/ha). *Quercus coccinea* had the highest volume of downed CWD (25.83 m^3 ha^{-1}), followed by *P. virginiana* (24.63 m^3 ha^{-1}) and *P. echinata* (16.09 m^3 ha^{-1}). We documented a density of 62 standing CWD individuals ha^{-1} and 219 downed CWD pieces ha^{-1}. Mean plot-level canopy openness was 35.5 % ± 1.0 % (SE), with a plot-level range of 25.3–47.4 %.

Residual tree basal area was 26.8 m^2/ha and density was 945 trees ha^{-1} (Table 2). Plot-level residual basal area was variable, ranging from 1.63 m^2 $plot^{-1}$ (32.60 m^2ha^{-1}) to 0.61 m^2 $plot^{-1}$ (12.23 m^2/ha). Of the 945 residual trees ha^{-1}, 559 were subcanopy *A. rubrum*, *O. arboreum*, and *I. opaca*. Of the residual canopy trees, we documented 132 residual *Pinus* individuals ha^{-1} and 118 *Quercus* individuals ha^{-1}. Residual tree species richness was 25 and Shannon diversity was 1.73. We documented 1632 saplings ha^{-1} and 87,703 seedlings ha^{-1} (Table 3). In the sapling layer, *A. rubrum* was the most abundant species, representing 52 % of saplings, followed by *I. opaca* (22 %) and *O. arboreum* (12 %). In the seedling layer, *A. rubrum* was most the abundant species, representing 46 % of seedlings, followed by *Vaccinium* spp. (12 %) and *Q. stellata* (5 %). Notably, *P. echinata* was absent in the sapling layer and minimally present in the seedling layer (Table 3; 1 % of seedlings). Species richness was 26 for saplings and 35 for seedlings. Shannon diversity was 1.22 for saplings and 1.59 for seedlings. The wind disturbance marginally increased mean tree diameter from 34.3 cm ± 10.6 (SE) pre-disturbance to 35.6 ± 9.2 (SE) post-disturbance. The spatial pattern of pre-disturbance trees (residual trees + snaps, snags, and uproots) was random (Fig. 2). Similarly, the spatial pattern of residual trees was random, which indicated that the disturbance had no effects on the spatial pattern of canopy trees.

3.2. Individual and neighborhood effects on survival probability

The random forest classification algorithm provided insight on the individual-tree and plot-level characteristics that influenced probability of survival. The final model had an OOB estimate of error rate of 23.7 %, live tree classification error of 19 %, dead tree classification error of 34 %, and AUC of 0.77. When the model was used to predict survival of the withheld test data, accuracy was 78 % ($p = 0.12$), Kappa index was 0.49, sensitivity was 0.85, and specificity was 0.65. The most importance

Table 2
Dominance (basal area; m^2ha^{-1}), relative dominance (%), density (stems ha^{-1}), relative density (%), and importance (average of relative dominance and importance) for all living trees ≥ 5 cm dbh in a wind-disturbed forest at Savage Gulf State Natural Area, TN, USA. Species are ranked by importance.

Species	Dominance (m^2ha^{-1})	Rel Dom (%)	Density (stems ha^{-1})	Rel Den (%)	Importance (%)
Acer rubrum L.	2.95	12	264	30	20.7
Pinus echinata Mill.	7.39	29	73	8	18.7
Oxydendrum arboreum (L.) DC.	3.08	12	193	22	16.9
Pinus virginiana Mill.	4.16	16	50	6	11.0
Quercus alba L.	2.56	10	79	9	9.5
Quercus coccinea Münchh.	1.88	7	13	1	4.4
Ilex opaca Aiton	0.24	1	67	8	4.3
Nyssa sylvatica Marshall	0.31	1	59	7	3.9
Carya tomentosa L.	0.68	3	39	4	3.5
Quercus rubra L.	0.65	3	6	1	1.6
Quercus velutina Lam.	0.51	2	6	1	1.4
Quercus stellata Wangenh.	0.33	1	7	1	1.0
Diospyros virginiana L.	0.10	0	9	1	0.7
Sassafras albidum (Nutt.) Nees	0.07	0	6	1	0.5
Liriodendron tulipifera L.	0.13	1	4	0	0.5
Quercus falcata Michx.	0.17	1	2	0	0.4
Fagus grandifolia Ehrh.	0.03	0	4	0	0.3
Prunus serotina Ehrh.	0.02	0	2	0	0.2
Carya glabra (Mill.) Sweet	0.02	0	2	0	0.2
Tsuga canadensis (L.) Carrière	0.04	0	1	0	0.1
Magnolia acuminata (L.) L.	0.01	0	1	0	0.1
Cornus florida L.	0.00	0	1	0	0.1
Crataegus spp.	0.00	0	1	0	0.0
TOTAL	**25.33**	**100**	**889.06**	**100**	**100.0**

Table 3
Density (stems ha^{-1}) and relative density (%) of seedlings (woody plants < 1 m height) and saplings (woody plants ≥ 1 m height; < 5 cm dbh) in a wind-disturbed forest at Savage Gulf State Natural Area, TN, USA. Species are ranked by relative density.

Species	Seedlings density (stems ha^{-1})	Rel Den (%)	Saplings density (stems ha^{-1})	Rel Den (%)
Acer rubrum L.	40359.4	46.0	841.7	51.6
Ilex opaca Aiton	2796.9	3.2	353.3	21.6
Oxydendrum arboreum (L.) DC.	625.0	0.7	188.3	11.5
Vaccinium elliottii Chapm.	6703.1	7.6	–	–
Quercus rubra L.	5078.1	5.8	–	–
Quercus coccinea Münchh.	4390.6	5.0	2.5	0.2
Nyssa sylvatica Marshall	1421.9	1.6	76.7	4.7
Quercus alba L.	3875.0	4.4	22.5	1.4
Quercus velutina Lam.	3703.1	4.2	6.7	0.4
Sassafras albidum (Nutt.) Nees	3562.5	4.1	20.8	1.3
Vaccinium stamineum L.	2906.3	3.3	23.3	1.4
Rhododendron periclymenoides (Michx.) Shinners	2906.3	3.3	0.8	0.1
Liriodendron tulipifera L.	2250.0	2.6	4.2	0.3
Pinus virginiana Mill.	1375.0	1.6	–	–
Diospyros virginiana L.	109.4	0.1	25.0	1.5
Pinus echinata Mill.	953.1	1.1	–	–
Vaccinium arboreum Marshall	953.1	1.1	3.3	0.2
Ilex montana Torr. & A. Gray ex A. Gray	937.5	1.1	12.5	0.8
Cornus florida L.	125.0	0.1	16.7	1.0
Carya tomentosa L.	718.8	0.8	14.2	0.9
Prunus serotina Ehrh.	515.6	0.6	0.8	0.1
Fagus grandifolia Ehrh.	–	–	5.0	0.3
Asimina triloba (L.) Dunal	234.4	0.3	–	–
Crataegus spp.	203.1	0.2	3.3	0.1
Quercus falcata Michx.	171.9	0.2	–	–
Ostrya virginiana (Mill.) K. Koch	109.4	0.1	2.5	0.2
Castanea dentata (Marshall) Borkh.	46.9	0.1	2.5	0.2
Quercus montana Willd.	125.0	0.1	–	–
Carya glabra (Mill.) Sweet	78.1	0.1	1.7	0.1
Quercus stellata Wangenh.	15.6	0.0	1.7	0.1
Magnolia acuminata (L.) L.	–	–	1.7	0.1
Hamamelis virginiana L.	46.9	0.1	–	–
Prunus americana Marshall	31.3	0.0	0.8	0.1
Carpinus caroliniana Walter	31.3	0.0	–	–
Callicarpa americana L.	15.6	0.0	–	–
TOTALS	**87375.0**	**100.0**	**1632.5**	**100.0**

predictor of survival was individual-tree basal area (MDG = 17.0; Fig. 3), followed by taxa (MDG = 16.6), and distance to nearest neighbor (MDG = 14.1). Overall, individual-tree predictor variables exhibited greater influence on survival probability than did aggregate plot-level variables (Fig. 3). The partial dependence plot of the influence of taxa on survival probability revealed that *Acer* spp. and *O. arboreum* were most likely to survive (75 % and 72 %, respectively; Fig. 4), and *P. echinata* and *P. virginiana* were least likely to survive (59 % and 46 %, respectively) the wind event. Nearly all taxa were more likely to survive than die (i.e., survival probability > 50 %) except *P. virginiana* (46 %, Fig. 4). The relationship revealed in the partial dependence plots of basal area and distance to nearest neighbor was non-linear, with little discernable pattern (Fig. 5). Trees with less basal area (e.g. smaller diameter trees) were more likely to survive from 0.02 m^2 to 0.05 m^2, with decreased survival probability from 0.05 m^2 to 0.09 m^2, and consistent survival probability of ca. 60 % with basal areas > 0.2 m^2 (Fig. 5). Trees with distance to nearest neighbor > 7 m were less likely to survive than trees with distance to nearest neighbor < 6 m, but this relationship was tenuous (Fig. 6).

3.3. Frequency, size, shape, and spatial distribution of detected canopy openings

The producer accuracy of the pixel-based supervised classification algorithm was 0.75 for forest pixels, 1.00 for bare ground pixels, and 0.89 for shadow pixels, and the Kappa index was 0.79. In the wind-disturbed mixed *Quercus-Pinus echinata* forest at SGNA, the classification algorithm identified a total of 1183 canopy openings (ca. 7 openings ha^{-1}; Fig. 7) that ranged in size from 50–7300 m^2 (Fig. 8). Based on the 200 m^2 canopy opening-size threshold, we documented 1047 small openings < 200 m^2 (ca. 6 openings ha^{-1}) and 136 large openings ≥ 200 m^2 (<1 opening ha^{-1}). The canopy openings-size frequency distribution exhibited a reverse-J pattern, with a higher frequency of small openings (50–150 m^2) and fewer large openings (Fig. 8). Specifically, we documented ca. 2 openings ha^{-1} in the 50–100 m^2 bin, 2 openings ha^{-1} in the 100–150 m^2 bin, and ca. 1 opening ha^{-1} in the 150–200 m bin. The remaining size class bins had < 0.5 openings ha^{-1}.

Mean area was 204 m^2 ± 355 (SD) for all openings, 135 m^2 ± 59 (SD) for small openings, and 734 m^2 ± 868 (SD) for large openings (Fig. 9). Mean perimeter was 153 m ± 206 (SD) for all openings, 109 m ± 45 (SD) for small openings, and 469 m ± 454 (SD) for large openings (Fig. 9). The largest detected opening perimeter was 3084 m and the smallest detected opening perimeter was 407 m. The mean perimeter area ratio was 0.82 ± 0.17 for all openings, 0.83 ± 0.17 for small openings, and 0.68 ± 0.12 for large openings (Fig. 9). The greater mean perimeter-area ratio of small openings compared to large openings indicated that, based on this shape complexity metric, small openings were more complex in shape. However, the shape complexity index was 1.35 ± 0.09 (SD) for all openings, 1.34 ± 0.08 (SD) for small openings, and 1.43 ± 0.07 (SD) for large openings (Fig. 9).

The general spatial pattern of canopy openings was significantly dispersed at short distances, and clustered at intermediate and greater distances (Fig. 10). This general pattern occurred for all openings and large openings, but small openings were randomly spatially distributed at greater distances. Specifically, all openings were significantly dispersed from 0 to 10 m and significantly clustered at distances from 20 to 250 m. Small openings exhibited a similar spatial distribution across the forest, with a significantly dispersed pattern documented from 0 to 10 m and a significantly clustered pattern from 30 to 100 m. Small openings were randomly distributed at distances > 100 m. For large openings, a significantly clustered spatial pattern was documented at distances from 10 to 120 m, followed by a random pattern from 120 to 200 m, and clustered pattern from 210 to 240 m.

4. Discussion

4.1. Composition, structure, and spatial patterns of woody plant mortality and survival

Intermediate-severity canopy disturbance often results in highly variable damage patterns as these events may create a high frequency of localized openings, few large openings, or some combination of canopy openings across a wide range of sizes (Hart and Kleinman 2018). We contend that ISD events are more frequent than commonly understood and may be more influential drivers of forest ecosystem change compared to gap-scale and stand-replacing disturbance (Nagel et al., 2017; Hart and Kleinman 2018). We noted that forest damage variability was high, with some portions of the disturbed forest exhibiting low-to moderate severity tree damage (i.e., few unique dead species and low

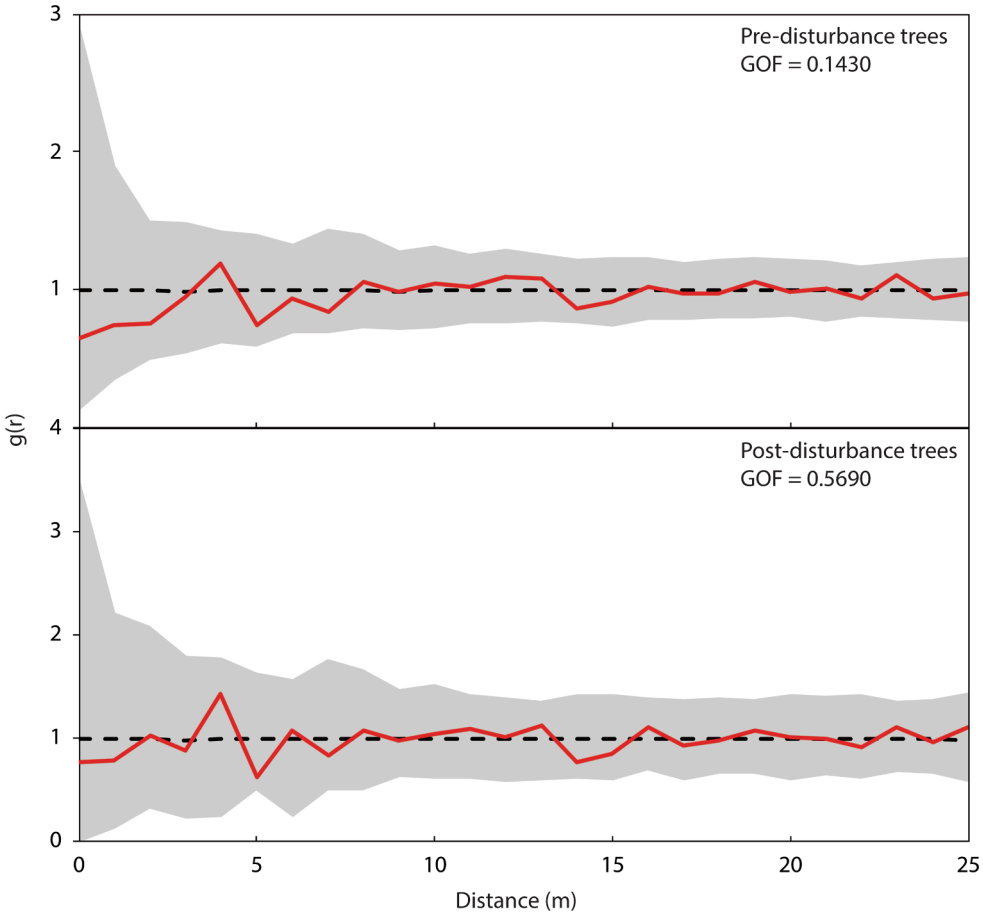

Fig. 2. Univariate pair correlation function *g (r)* for reconstructed pre-disturbance trees (top panel) and post-disturbance residual trees (bottom panel) following a November 2018 intermediate-severity wind disturbance in Savage Gulf State Natural Area, TN, USA. Shaded areas represent a 95 % confidence envelope (99 permutations excluding the five highest and lowest values) simulated under the assumption of complete spatial randomness (CSR). The red line is observed values. Values above the gray shaded area indicate significant ($p < 0.05$) clustering (i.e., trees were closer in space than expected when compared to tree locations simulated under the assumption of CSR), and values below the shaded area represent significant dispersion. Goodness-of-fit (GoF) for each *g(r)* is reported in the top right of each panel. (For interpretation of the references to color in this figure legend, the reader is referred to the web version of this article.)

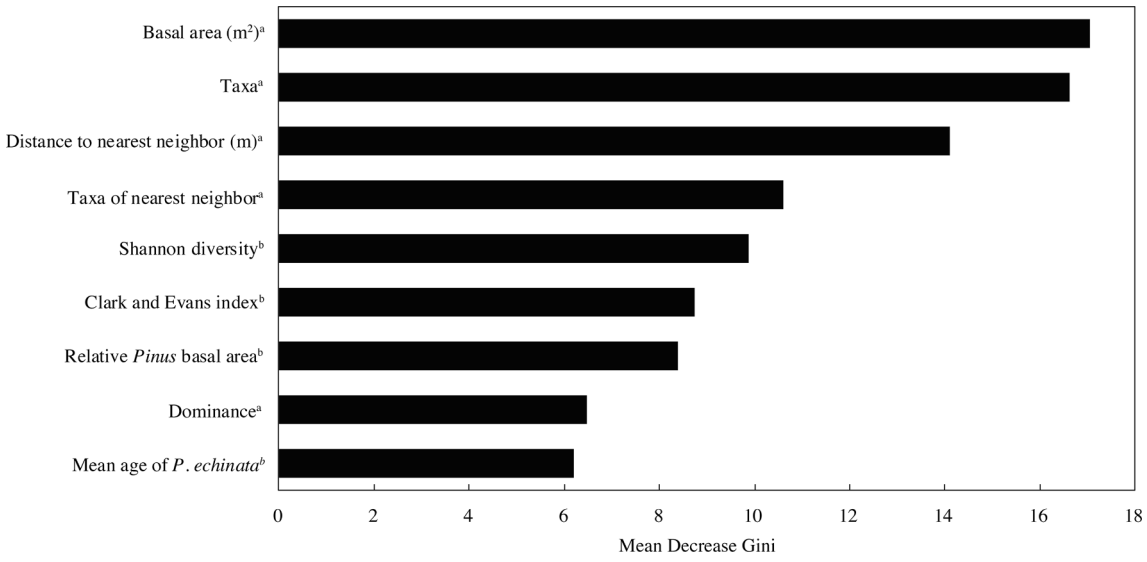

Fig. 3. Random forest classification algorithm variable importance rankings for the influence of individual-tree metrics (a) and neighborhood characteristics (b) on individual-tree survival probability following a November 2018 intermediate-severity wind disturbance in Savage Gulf State Natural Area, TN, USA. Mean decrease Gini values indicate the total decrease in node impurity averaged over all classification trees. Greater mean decrease Gini values for a given predictor indicate greater importance. The Clark and Evans index is a crude measure of aggregation of a point pattern, with values > 1 indicating random pattern and values < 1 indicating clustered pattern. Dominance is a spatially-explicit competition metric that quantifies the diameter differentiation of a five tree neighborhood.

diversity in mode of death), and some portions of the forest exhibiting high-severity tree damage (i.e., large number of unique dead species and high diversity in mode of death; Peterson 2019). The severe thunderstorm that impacted the SGNA produced strong downbursts that damaged a relatively large area (NOAA Storm Events Database 2022). Imbedded within downbursts are microbursts, which are discreet high severity wind gusts that result in concentrated patches of tree mortality (Peterson et al., 2016). Similar patterns of canopy tree damage were

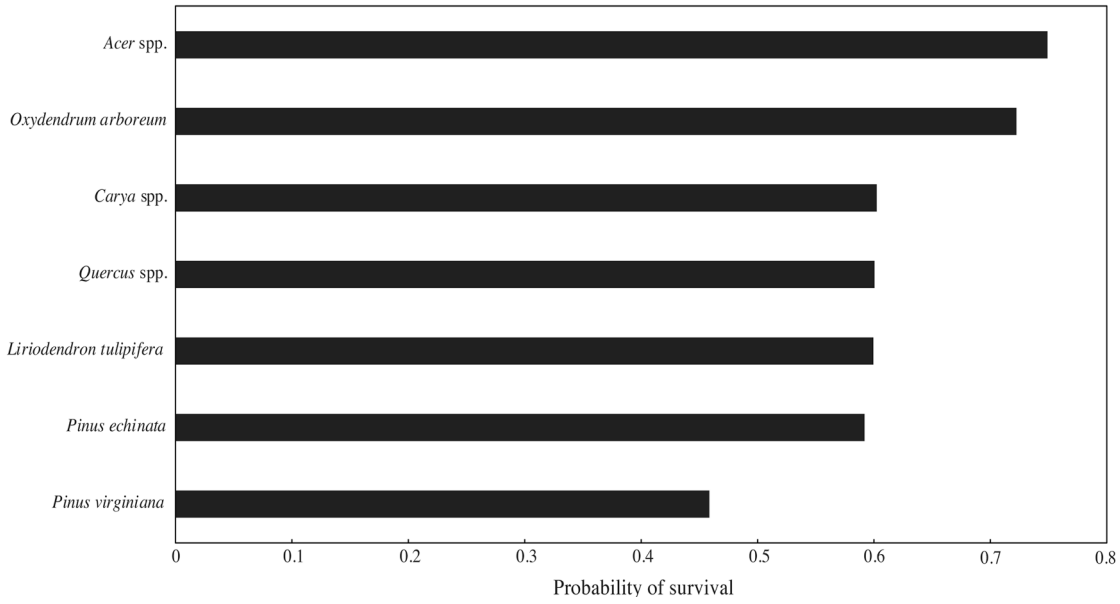

Fig. 4. Partial dependence plot estimating the probability of survival as influenced by tree taxon following a November 2018 intermediate-severity wind disturbance in Savage Gulf State Natural Area, TN, USA. Partial dependence plot depicts the influence of tree taxon on the likelihood of tree survival based on balanced random forest classification algorithm when all other predictor variables are held constant.

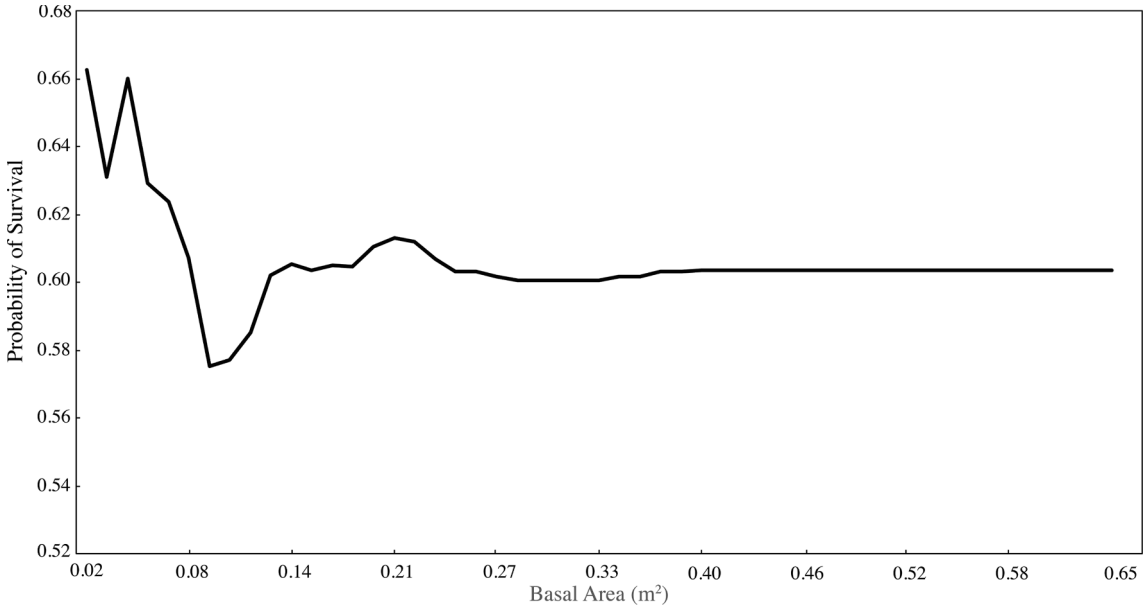

Fig. 5. Partial dependence plot estimating the probability of survival as influenced by individual-tree basal area (m^2) following a November 2018 intermediate-severity wind disturbance in Savage Gulf State Natural Area, TN, USA. Partial dependence plot depicts the influence of basal area (m^2) on the likelihood of tree survival based on balanced random forest classification algorithm when all other predictor variables are held constant.

documented from hurricane-produced downbursts in upland *Quercus* forests in North Carolina (Greenberg and McNab 1998), in which the damage was associated with multiple discreet downburst events produced from the same storm system. Similarly, disturbance-induced tree mortality was documented in an upland *Quercus* stand in Alabama following a low-intensity EF-1 tornado (Cox et al., 2016), in which large stems were disproportionately removed from the canopy in the lightly and moderately disturbed portions of the stand.

In damaged portions of the forest, basal area lost and CWD volume was highly variable. These findings corresponded to other investigations of intermediate-severity canopy disturbances in temperate forests of the eastern United States (Woods 2004; Hanson and Lorimer 2007; Busing et al., 2008; Holzmueller et al. 2012; Trammell et al., 2017). The CWD volume ha^{-1} documented after intermediate-severity disturbance was well above the background CWD inputs reported on relatively undisturbed sites on the Cumberland Plateau (Muller and Liu 1991). We documented relatively high residual basal area (26.8 m^2ha^{-1}) and tree density (945 stems ha^{-1}), which could be attributed to the relatively high basal area and tree density of the pre-disturbance forest. But similar to CWD metrics discussed above, we documented a wide range of variability in plot-level residual basal area and tree density. Canopy openness was also highly variable, which was likely influenced by midstory tree and sapling density, as hemispherical photographs were captured from 1 m height. Although the wind-disturbance removed

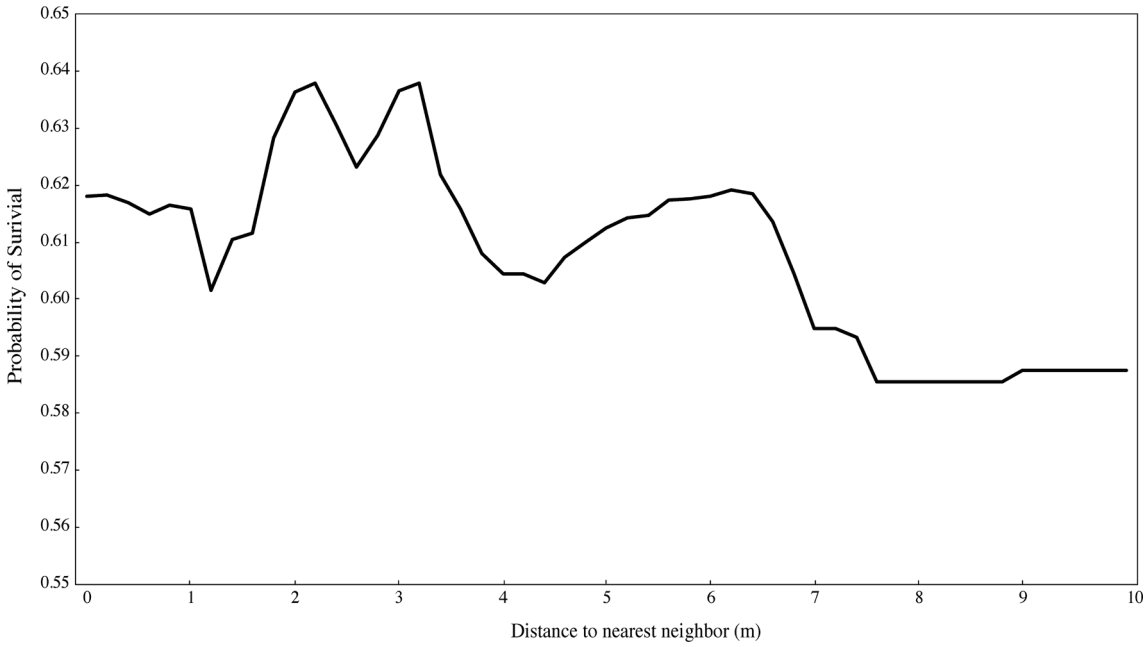

Fig. 6. Partial dependence plot estimating the probability of survival as influenced by distance to nearest neighbor (m) following a November 2018 intermediate-severity wind disturbance in Savage Gulf State Natural Area, TN, USA. Partial dependence plot depicts the influence distance to nearest neighbor (m) on the likelihood of tree survival based on balanced random forest classification algorithm when all other predictor variables are held constant.

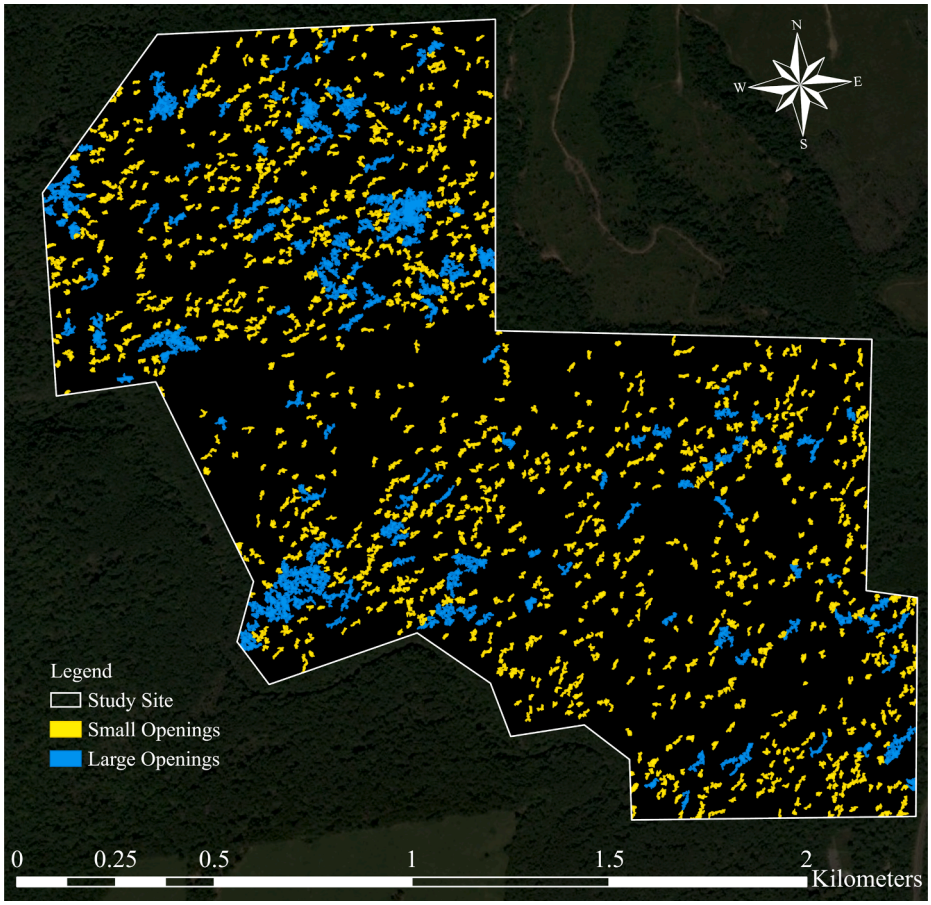

Fig. 7. Study area map (174 ha) showing the distribution of detected small (yellow; < 200 m^2) and large (blue; ≥ 200 m^2) canopy openings following a November 2018 intermediate-severity wind disturbance in Savage Gulf State Natural Area, TN, USA. (For interpretation of the references to color in this figure legend, the reader is referred to the web version of this article.)

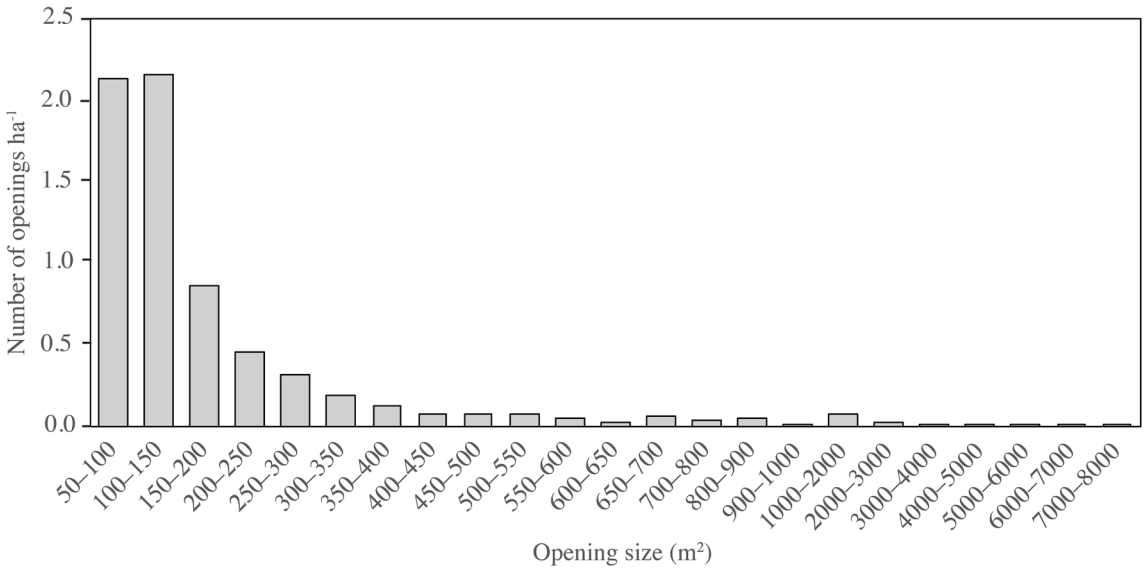

Fig. 8. Canopy opening size-frequency distribution of detected canopy openings following a November 2018 intermediate-severity wind disturbance in Savage Gulf State Natural Area, TN, USA.

mature canopy trees, most potential understory light was captured by the dense midstory of shade-tolerant taxa (Hanson and Lorimer, 2007; Cowden et al., 2014; Meigs and Keeton, 2018).

Surviving trees exhibited a significantly random spatial pattern through the damaged portions of the forest. Pre-disturbance canopy tree locations were spatially random, and the canopy disturbance did not alter this spatial pattern. Although species, neighborhood, and site-specific variables influence patterns of canopy tree mortality, ISD has been found to result in random horizontal spatial patterns of surviving individuals (Boutet and Weishampel, 2003; Stueve et al., 2011). We suspect that with increased disturbance severity, spatial patterns of residual trees would likely become either aggregated or dispersed depending on the canopy disturbance mechanism. For example, high severity, catastrophic wind disturbance may result in clustered spatial patterns of mortality (Foster and Boose 1992; Cannon et al., 2016). Biotic disturbance agents (e.g. insects) may results in dispersed patterns of mortality, but these patterns may manifest at different spatial scales across neighborhoods, stands, and forests (Frelich and Reich 1999; Woods 2004). However, the documented random spatial patterns could be a function of truncating and combining individual circular plots, which has been found to result in lack of spatial clustering or dispersion in other studies (see Gray et al. 2021).

4.2. Individual and neighborhood effects on survival probability

The RF classifier identified the most influential individual-tree and site characteristics on individual-tree survival. Taxon was an influential predictor of survival, which was driven by the diversity of life history strategies and functional traits of documented taxa. Specifically, midstory shade-tolerant *A. rubrum* and *O. arboreum* were more likely to survive based on subcanopy location in the vertical strata. *Acer rubrum* and *O. arboreum* are commonly abundant in the midstory of upland *Quercus* and *Quercus-Pinus* stands (Hart et al. 2012; Vander Yacht et al., 2017). Survival of these species was most likely associated with canopy position, diameter, and buffering effects from canopy trees (Greenberg 2021). These species were more likely buffered from the wind damage by the overtopping canopy stratum. Midstory stems are not typically damaged directly by wind, but by the falling crowns of canopy trees (Brokaw 1985), or the entanglement of root networks from neighboring uprooted canopy stems.

We found a negative relationship between individual-tree basal area and probability of survival. This finding is congruent with a robust literature on the relationship between tree size and mortality (Peterson et al., 2016; Salas-Eljatib and Weiskittel, 2020). Tree diameter is positively related to tree height, and trees situated in higher canopy strata are exposed to greater wind speeds. The documented basal area-survival relationship in our study revealed a peak probability of survival at small basal areas (i.e., small diameters), which is a commonly reported trend in the literature (e.g. Everham and Brokaw, 1996; White et al., 2015). The nadir of survival probability occurred at basal areas of 0.09–0.11 m^2, and plateaued at basal areas > 0.14 m^2 (ca. 42 cm dbh). Although smaller individuals were more likely to survive, the range in survival probability was < 10 % across all basal areas. We documented a weak, non-linear relationship between distance to nearest neighbor and survival probability, although this finding may be confounded by edge effects. Few studies have examined spatially-explicit neighborhood effects on tree survival probability (Peterson and Cannon 2021), such as distance to nearest neighbor (but see Gonzalez-Akre et al., 2016; Hülsmann et al. 2018). The importance of spatially-explicit, neighborhood-scale predictor variables may aid the predictive ability of windthrow susceptibility models.

We found that individual-tree characteristics (e.g. basal area, taxa) were more influential on survival than plot-level characteristics (Bakaj et al. 2016). In order of importance, basal area, taxa, and distance to nearest neighbor exerted the greatest influence on tree survival. The plot-level variables selected were hypothesized to be more influential on survival, but these relationships were tenuous and explained relatively little variance compared to individual-tree predictors. Each of the plot-level predictors had a similar MDG (range 6.1–10.0). Individual trees on plots with greater Shannon diversity were marginally more likely to survive. A similar pattern was documented with plot-level relative *Pinus* spp. basal area and mean age. Mixed-species stands have been hypothesized to be more resistant to disturbance (Griess and Knoke, 2011; Panayotov et al., 2011; Kabrick et al., 2017) and our results provide some, albeit weak, support for this hypothesis. For example, we expect that individual trees on plots with greater *Pinus* spp. basal area or tree-level Shannon diversity would experience marginally greater resistance to mortality from a strong wind event. Our classification algorithm confirmed this hypothesis, although these weak relationships were non-linear. Future research should explicitly test the hypothesis that management for both hardwoods and softwoods does indeed enhance ecosystem resilience and resistance to disturbance, including wind events. Although we did document this pattern, windthrow resistance in this *Quercus-P. echinata* stand was more so a function of individual-tree

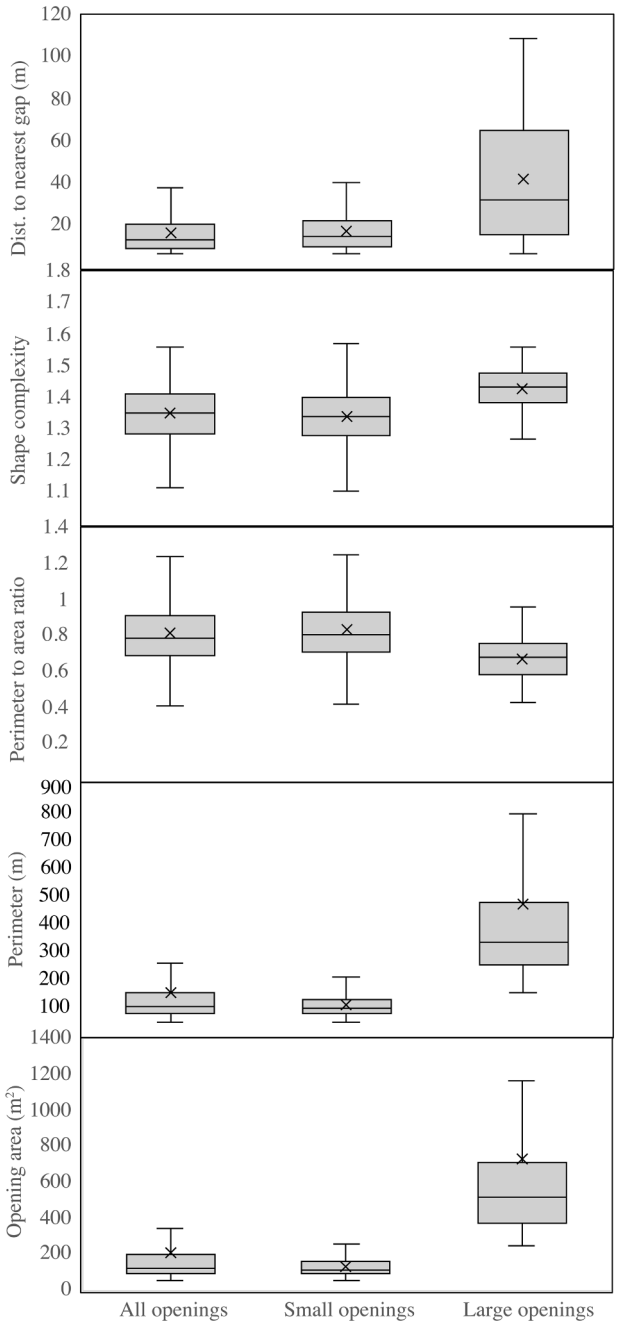

Fig. 9. Boxplots of canopy opening metrics calculated with the "landscapemetrics" package in R for all openings, small openings (<200 m^2), and large openings (≥200 m^2). Distance to nearest opening is the mean edge-to-edge distance between openings in meters. Shape complexity is a scale-independent, standardized metric based on the perimeter and area of openings, with values ranging from 1 (least complex shape) to 2 (most complex shape). Canopy openings were detected from orthoimagery using remote sensing techniques following a November 2018 intermediate-severity wind disturbance in Savage Gulf State Natural Area, TN, USA.

characteristics and less so of neighborhood conditions. However, our analysis of individual-tree mortality was among the few to incorporate both individual-tree characteristics and spatially-explicit neighborhood conditions (Peterson and Cannon 2021). We suggest that future studies incorporate abiotic site conditions as windthrow susceptibility predictor variables, such as soil depth, underlying geology, and microtopography.

4.3. Frequency, size, shape, and spatial patterns of detected canopy openings

We detected many small canopy openings and frequency decreased with increased opening size. These results conform to gap size-frequency distributions documented in several other intermediate-severity wind disturbance studies of tornados in *P. palutris* stands (Cannon et al., 2016) and *Quercus-Carya* stands (Rebertus and Meier 2001), and severe thunderstorm winds in northern hardwood stands (Evans et al. 2007), among others (see Foster and Boose 1992; Curzon and Keeton 2010; Panayotov et al. 2011). These patterns are hypothesized to be a result of variable disturbance intensity. The intensity of wind events is often relatively low over the extent of the atmospheric disturbance, and high-intensity sub-events are imbedded over smaller areas (e.g. microbursts in large thunderstorm systems). Furthermore, storm intensity is not always related to damage severity (Peterson 2000) as abiotic factors such as topographic features (Cannon et al., 2016), tree structure and morphological traits (e.g. Brisson 2001), and landscape characteristics (e.g. distance to edge, Stueve et al., 2011) influence storm-related damage.

Detected canopy openings ranged in size from 50–7300 m^2. This is a smaller range of canopy opening sizes than what some other studies have reported after hurricane (Boutet and Weishampel, 2003; McNab et al., 2004; Busing et al., 2008) and tornado disturbances (Peterson et al. 2016; Rebertus and Meier 2001). We found that larger openings had a greater shape complexity (i.e., less square), but smaller openings had a greater mean perimeter-area ratio (i.e., more edge length). However, perimeter-area ratios were less than those reported from canopy gap analyses in mature Mediterranean *Fagus* stands (Solano et al., 2022), which could indicate the canopy opening shapes are more complex in older stands when analyzed across a broader temporal scale. Therefore, both large and small openings exhibited complex shapes and the discrepancy between metrics was likely a function of the pixel-based classification. Structural heterogeneity may be enhanced by openings that exhibit high shape complexity or perimeter-area ratios (Canham et al., 1994). We suspect that stands with high canopy tree species richness and a wide range of canopy tree size classes favor greater shape complexity and perimeter-area ratio of canopy openings. Although our study design did not permit testing of this potential relationship, we hypothesize that damage diversity is positively related to canopy opening shape complexity.

Large canopy openings are one component required for establishment and recruitment *P. echinata* (Goode et al. 2021), and the return interval of ISD events is often shorter than the lifespan of most canopy trees. We found that larger openings (i.e., those ≥ 200 m^2) were spatially clustered within the forest studied here at distances of 10–120 and 210–240 m. The spatial pattern of large openings was likely a function of the wind event, as microbursts may result in clustered canopy openings (Hjelmfelt et al., 2010; Gospodinov et al., 2015), and these patterns have been documented in many forest types and across different disturbance agents. Van der Meer and Bongers (1996) found clustered patterns of small-canopy gaps around large gaps in tropical forests, which was explained by site factors and wind exposure. In subtropical forests of China, Liu et al. (2020) found that canopy gaps following ice storm damage were clustered at distances > 70 m. Curzon and Keeton (2010) found clustering of canopy gaps in *Tsuga canadensis*- northern hardwood stands and McNab et al. (2004) found clusters of large canopy openings following hurricane disturbance in stands of the Appalachian Highlands. In addition to storm-related characteristics, a range of biophysical site conditions may also explain the underlying mechanisms of opening patterns including topography, soil conditions or neighborhood effects (Poorter et al., 1994).

4.4. Management implications

Our findings provide quantitative information on natural canopy

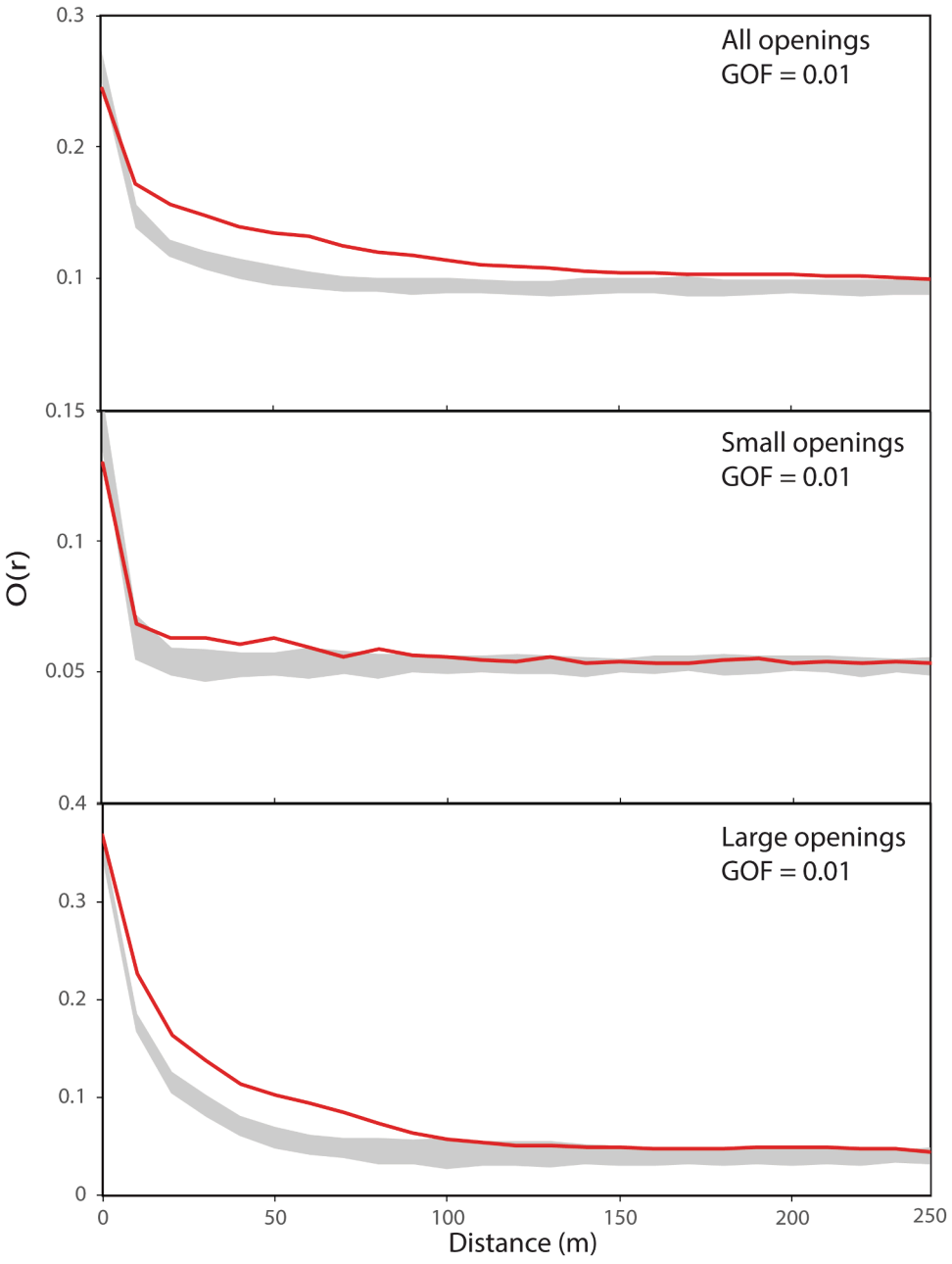

Fig. 10. Univariate O-ring function *O(r)* for all openings (top panel), small openings (<200 m^2; middle panel) and large openings (≥200 m^2; bottom panel) following a November 2018 intermediate-severity wind disturbance in Savage Gulf State Natural Area, TN, USA. Point-pattern analysis was adapted for objects with finite size and real shape (i.e., canopy openings). Shaded areas represent a 95 % confidence envelope (99 permutations excluding the five highest and lowest values) simulated under the assumption of complete spatial randomness (CSR). The red line is observed values. Values above the gray shaded area indicate significant ($p < 0.05$) clustering (i.e., openings were closer in space than expected when compared to opening locations simulated under the assumption of CSR), and values below the shaded area represent significant dispersion. Goodness-of-fit (GOF) for each *O(r)* is reported in the top right of each panel. (For interpretation of the references to color in this figure legend, the reader is referred to the web version of this article.)

disturbances in *Quercus-Pinus* mixedwoods and can be used to inform silvicultural systems that emulate natural disturbance and development patterns that sustain mixedwood forests. We found individual canopy openings were typically 50–7500 m^2 in size and all canopy openings were typically irregular in shape. For single-tree gaps (i.e., openings of < 200 m^2), we documented a frequency of five openings ha^{-1}, and these openings were spatially clustered at distances of 30–100 m and randomly distributed at distances > 100 m. Large openings of over 1000 m^2 had a frequency of 0.14 ha^{-1}. On average, there was one canopy opening of at least 200 m^2 for every 0.6 ha and openings of at least 200 m^2 were spatially clustered from 10 to 120 m and 210–240 m. Although large openings on average occurred at a frequency of one per 0.6 ha, they were not uniformly distributed across the forest; rather, they were concentrated in patches (i.e., a clustered group of canopy openings). These concentrated patches of canopy openings could occur as few relatively large openings or up to five intermediate-sized openings. Spatial analysis of canopy openings indicated that the edge-to-edge distance between them was significantly less than expected when compared to openings simulated under the assumption of complete spatial randomness. Within canopy openings, ca. 50 % of trees ≥ 15 cm dbh survived, and these trees were randomly distributed in space (i.e., not aggregated or dispersed).

In *Quercus-Pinus* mixedwood stands, the perpetuation of the *Pinus* component is paramount (Kenefic et al. 2021). Silvicultural systems that promote *Pinus* regeneration and are aligned with the natural patterns of canopy disturbance documented here would include patch seedtree harvests with reserves or irregular shelterwood harvests with an emphasis on the retention of sexually mature *P. echinata,* or patch clearcut harvests with reserves in neighborhoods that lack mature *Pinus* individuals, but where abiotic conditions indicate *Pinus* may be able to regenerate naturally and be competitive (e.g., sandy, nutrient poor sites). In addition to *Pinus* stems, reserve trees in openings could be those that produce fire-facilitating fuels to maintain desired fire effects throughout the rotation. We recommend that harvest-created openings

be up to 0.75 ha and be clustered in groups of 2–5 openings with an edge-to-edge distance between openings of < 200 m. We acknowledge that canopy disturbances must be coordinated in conjunction with prescribed fire and possibly other treatments, such as chemical and mechanical competition control, to regenerate and maintain *P. echinata*. Outplanting of *P. echinata* in large harvest-created openings may be necessary even when mature *P. echinata* trees are present to supplement natural regeneration and would of course be required in openings that lacked a *Pinus* seed source. Regardless of the approach used, we recommend entries be spatially clustered and variable in size to emulate the patterns of the natural disturbance documented here.

Ethics approval and consent to participate

Not applicable.

Consent for publication

Not applicable.

Availability of data and material

The datasets used and analyzed during the current study are available from the corresponding author upon reasonable request.

Funding

This project was funded through a Joint Venture Agreement between the Northern Research Station, USDA Forest Service, and the University of Alabama (18-JV-1242311-073) and the U.S. National Science Foundation award number 2224894.

CRediT authorship contribution statement

J. Davis Goode: Conceptualization, Methodology, Data curation, Formal analysis, Writing – original draft. **Anuska Narayanan:** Formal analysis, Writing – review & editing. **David L. Phillips:** Data curation, Methodology, Writing – original draft. **Justin L. Hart:** Conceptualization, Methodology, Writing – original draft. **Scott J. Torreano:** Conceptualization, Resources, Writing – review & editing. **Daniel C. Dey:** Conceptualization, Funding acquisition, Writing – original draft.

Declaration of Competing Interest

The authors declare that they have no known competing financial interests or personal relationships that could have appeared to influence the work reported in this paper.

Data availability

Data will be made available on request.

Acknowledgements

This project was funded through a Joint Venture Agreement between the Northern Research Station, USDA Forest Service, and the University of Alabama. We thank Campbell Taylor and R.L. England for assistance in the field; Brady Allen, Lucas Hales, Jon Kiep, and Christal Varanyak for assistance in the lab. We thank Roger McCoy and Murray Gheesling from the Tennessee Department of Environment and Conservation, and Aaron Reid from Tennessee State Parks for sampling permits and logistical support.

References

Aguirre, O., Hui, G., von Gadow, K., Jiménez, J., 2003. An analysis of spatial forest structure using neighbourhood-based variables. For. Ecol. Manage. 183 (1–3), 137–145.

ESRI ArcGIS Pro version 2.9 (2022). Esri Inc. https://www.esri.com/en-us/arcgis/products/arcgis-pro/overview.

Axelson, J.N., Alfaro, R.I., Hawkes, B.C., 2010. Changes in stand structure in uneven-aged lodgepole pine stands impacted by mountain pine beetle epidemics and fires in central British Columbia. Forestry Chronicle 86 (1), 87–99.

Baddeley, A., Turner, R., 2005. Spatstat: an R package for analyzing spatial point patterns. J. Stat. Softw. 12, 1–42.

Baddeley, A., Rubak, E., Turner, R., 2015. Spatial point patterns: methodology and applications with R. CRC Press.

Bakaj, F., Mietkiewicz, N., Veblen, T.T., Kulakowski, D., 2016. The relative importance of tree and stand properties in susceptibility to spruce beetle outbreak in the mid-20th century. Ecosphere 7 (10).

Battles, J.J., Cleavitt, N.L., Saah, D.S., Poling, B.T., Fahey, T.J., 2017. Ecological impact of a microburst windstorm in a northern hardwood forest. Can. J. For. Res. 47 (12), 1695–1701.

Beers, T.W., Dress, P.E., Wensel, L.C., 1966. Notes and observations: aspect transformation in site productivity research. J. Forest. 64 (10), 691–692.

Boutet, J.C., Weishampel, J.F., 2003. Spatial pattern analysis of pre-and post-hurricane forest canopy structure in North Carolina, USA. Landscape Ecol. 18 (6), 553–559.

Brisson, J., 2001. Neighborhood competition and crown asymmetry in Acer saccharum. Can. J. For. Res. 31 (12), 2151–2159.

Brokaw, N.V.L., 1985. Treefall, regrowth, and community structure in tropical forests. In: Pickett, S.T.A., White, P.S. (Eds.), The ecology of natural disturbance and patch dynamics.

Busing, R.T., White, R.D., Harmon, M.E., White, P.S., 2008. Hurricane disturbance in a temperate deciduous forest: patch dynamics, tree mortality, and coarse woody detritus. In *Forest Ecology*. In: Van der Valk, A.G. (Ed.), Forest Ecology. Springer Netherlands, Dordrecht, pp. 351–363.

Canham, C.D., Finzi, A.C., Pacala, S.W., Burbank, D.H., 1994. Causes and consequences of resource heterogeneity in forests: interspecific variation in light transmission by canopy trees. Can. J. For. Res. 24 (2), 337–349.

Canham, C.D., Papaik, M.J., Latty, E.F., 2001. Interspecific variation in susceptibility to windthrow as a function of tree size and storm severity for northern temperate tree species. Can. J. For. Res. 31 (1), 1–10.

Cannon, J.B., Hepinstall-Cymerman, J., Godfrey, C.M., Peterson, C.J., 2016. Landscape-scale characteristics of forest tornado damage in mountainous terrain. Landscape Ecol. 31 (9), 2097–2114.

Chen, C., Liaw, A., Breiman, L., 2004. Using random forest to learn imbalanced data. Univ. California, Berkeley 110 (1–12), 24.

Clark, P.J., Evans, F.C., 1954. Distance to nearest neighbor as a measure of spatial relationships in populations. Ecology 35 (4), 445–453.

Cooper, A.W., 1989. Ecology of the pine-hardwood type. In: Proc. of Pine-hardwood mixtures: A symposium on management and ecology of the type (pp. 3-8). USDA Forest Service Gen. Tech. Rep. SE-58, Southeastern Forest Experiment Station, Asheville, NC.

Covey, K.R., Barrett, A.L., Ashton, M.S., 2015. Ice storms as a successional pathway for Fagus grandifolia advancement in Quercus rubra dominated forests of southern New England. Can. J. For. Res. 45 (11), 1628–1635.

Cowden, M.M., Hart, J.L., Schweitzer, C.J., Dey, D.C., 2014. Effects of intermediate-scale wind disturbance on composition, structure, and succession in Quercus stands: Implications for natural disturbance-based silviculture. For. Ecol. Manage. 330, 240–251.

Cox, L.E., Hart, J.L., Dey, D.C., Schweitzer, C.J., 2016. Composition, structure, and intra-stand spatial patterns along a disturbance severity gradient in a Quercus stand. For. Ecol. Manage. 381, 305–317.

Curzon, M.T., Keeton, W.S., 2010. Spatial characteristics of canopy disturbances in riparian old-growth hemlock–northern hardwood forests, Adirondack Mountains, New York, USA. Can. J. For. Res. 40 (1), 13–25.

Daniels, M.K., Larson, E.R., Jucker, T., 2020. Effects of forest windstorm disturbance on invasive plants in protected areas of southern Illinois, USA. J. Ecol. 108 (1), 199–211.

Evans, A.M., Camp, A.E., Tyrrell, M.L., Riely, C.C., 2007. Biotic and abiotic influences on wind disturbance in forests of NW Pennsylvania, USA. For. Ecol. Manage. 245 (1–3), 44–53.

Everham, E.M., Brokaw, N.V., 1996. Forest damage and recovery from catastrophic wind. The Botanical Rev. 62 (2), 113–185.

Fenneman, N.M., 1938. Physiography of Eastern United States. McGraw-Hill Book Company, New York.

FIA, 2005. Forest Inventory and Analysis National Program. (2005). 3.0 Phase 3 Field Guide – Down Woody Materials, 1–38.

Foster, D.R., Boose, E.R., 1992. Patterns of forest damage resulting from catastrophic wind in central New England, USA. J. Ecol. 80 (1), 79.

Foster, D.R., Motzkin, G., Slater, B., 1998. Land-use history as long-term broad-scale disturbance: regional forest dynamics in central New England. Ecosystems 1 (1), 96–119.

Fraver, S., Ringvall, A., Jonsson, B.G., 2007. Refining volume estimates of down woody debris. Can. J. For. Res. 37 (3), 627–633.

Frelich, L., 2016. Forest dynamics [version 1; peer review: 2 approved]. F1000Research 2016, 5(F1000 Faculty Rev):183 (https://doi.org/10.12688/f1000research.7412.1).

Frelich, L.E., Reich, P.B., 1995. Spatial patterns and succession in a Minnesota southern-boreal forest. Ecol. Monogr. 65 (3), 325–346.
Frelich, L.E., Reich, P.B., 1999. Minireviews: neighborhood effects, disturbance severity, and community stability in forests. Ecosystems 2 (2), 151–166.
Fulé, P.Z., Crouse, J.E., Heinlein, T.A., Moore, M.M., Covington, W.W., Verkamp, G., 2003. Mixed-severity fire regime in a high-elevation forest of Grand Canyon, Arizona, USA. Landscape Ecol. 18 (5), 465–486.
Gonzalez-Akre, E., Meakem, V., Eng, C.-Y., Tepley, A.J., Bourg, N.A., McShea, W., Davies, S.J., Anderson-Teixeira, K., 2016. Patterns of tree mortality in a temperate deciduous forest derived from a large forest dynamics plot. Ecosphere 7 (12), e01595.
Goode, J.D., Hart, J.L., Dey, D.C., Torreano, S.J., Clark, S.L., 2021. Spatial Patterns of Canopy Disturbance and Shortleaf Pine in a Mixedwood Forest. Forest Sci. 67(4), 433-445.
Gospodinov, I., Dimitrova, T., Bocheva, L., Simeonov, P., Dimitrov, R., 2015. Derecho-like event in Bulgaria on 20 July 2011. Atmos. Res. 158, 254–273.
Gray, A.N., McIntosh, A.C.S., Garman, S.L., Shettles, M.A., 2021. Predicting canopy cover of diverse forest types from individual tree measurements. For. Ecol. Manage. 501, 119682.
Greenberg, C.H., 2021. Long-term recovery dynamics following hurricane-related wind disturbance in a southern Appalachian forest. For. Ecol. Manage. 502, 119704.
Greenberg, C.H., McNab, W.H., 1998. Forest disturbance in hurricane-related downbursts in the Appalachian mountains of North Carolina. For. Ecol. Manage. 104 (1–3), 179–191.
Greenwell, B.M., 2017. pdp: an R Package for constructing partial dependence plots. The R Journal 9 (1), 421.
Griess, V.C., Knoke, T., 2011. Growth performance, windthrow, and insects: meta-analyses of parameters influencing performance of mixed-species stands in boreal and northern temperate biomes. Can. J. For. Res. 41 (6), 1141–1159.
Habashi, H., 2019. Spatial correlation of pit and mound topography with canopy gaps in a virgin mixed beech forest, northern Iran. J. For. Res. 30 (1), 295–303.
Hanson, J.J., Lorimer, C.G., 2007. Forest structure and light regimes following moderate wind storms: Implications for multi-cohort management. Ecol. Appl. 17 (5), 1325–1340.
Hart, J.L., Clark, S.L., Torreano, S.J., Buchanan, M.L., 2012. Composition, structure, and dendroecology of an old-growth Quercus forest on the tablelands of the Cumberland Plateau, USA. For. Ecol. Manage. 266, 11–24.
Hart, J.L., Cox, L.E., 2017. Incorporating intermediate-severity disturbances in oak stand development. Forests 8 (8), 284.
Hart, J.L., Kleinman, J.S., 2018. What are intermediate-severity forest disturbances and why are they important? Forests 9 (9), 579.
Hart, J.L., Kupfer, J.A., 2011. Sapling richness and composition in canopy gaps of a southern Appalachian mixed Quercus forest1. J. Torrey Botanical Society 138 (2), 207–219.
Hesselbarth, M.H., Sciaini, M., With, K.A., Wiegand, K., Nowosad, J., 2019. landscapemetrics: An open-source R tool to calculate landscape metrics. Ecography 42 (10), 1648–1657.
Hinkle, C.R., 1978. The relationship of forest communities and selected species to edaphic and topographic factors on the Cumberland Plateau of Tennessee. University of Tennessee, Knoxville. Doctoral dissertation,.
Hinkle, C.R., 1989. Forest communities of the Cumberland Plateau of Tennessee. J. Tenn. Acad. Sci. 64, 123–129.
Hjelmfelt, M.R., Johnson, E.A., Miyanishi, K., 2010. Microbursts and macrobursts: windstorms and blowdowns. Academic Press, Burlington, Massachusetts, pp. 59–101.
Hobi, M.L., Ginzler, C., Commarmot, B., Bugmann, H., 2015. Gap pattern of the largest primeval beech forest of Europe revealed by remote sensing. Ecosphere 6 (5), 1–15.
Holzmueller, E.J., Gibson, D.J., Suchecki, P.F., 2012. Accelerated succession following an intense wind storm in an oak-dominated forest. For. Ecol. Manage. 279, 141–146.
Hosmer, D.W., Lemesbow, S., 1980. Goodness of fit tests for the multiple logistic regression model. Commun. Statist.-Theory Methods 9 (10), 1043–1069.
Hülsmann, L., Bugmann, H., Cailleret, M., Brang, P., 2018. How to kill a tree: empirical mortality models for 18 species and their performance in a dynamic forest model. Ecol. Appl. 28 (2), 522–540.
Kabrick, J.M., Clark, K.L., D'Amato, A.W., Dey, D.C., Kenefic, L.S., Kern, C.C., Knapp, B. O., MacLean, D.A., Raymond, P., Waskiewicz, J.D., 2017. Managing hardwood-softwood mixtures for future forests in eastern North America: Assessing suitability to projected climate change. J. Forest. 115 (3), 190–201.
Kenefic, L.S., Kabrick, J.M., Knapp, B.O., Raymond, P., Clark, K.L., D'Amato, A.W., Kern, C.C., Vickers, L.A., Dey, D.C., Rogers, N.S., 2021. Mixedwood silviculture in North America: the science and art of managing for complex, multi-species temperate forests. Can. J. For. Res. 51 (7), 921–934.
Lawrence, B., 2022. Classifying Forest Structure of Red-Cockaded Woodpecker Habitat Using Structure from Motion Elevation Data De-Rived from sUAS Imagery. Drones 6 (1), 26.
Lawson, E.R., Kitchens, R.N., 1983. Shortleaf pine. *Burns, RM tech. compiler. Silvicultural systems for the major forest types of the United States*. Agric. Hndbk 445, 157–161.
Liaw, A., Wiener, M., 2002. Classification and regression by randomForest. R news 2 (3), 18–22.
Liu, F., Yang, Z.G., Zhang, G., 2020. Canopy gap characteristics and spatial patterns in a subtropical forest of South China after ice storm damage. J. Mountain Sci. 17 (8), 1942–1958.
McGarigal, K., Cushman, S.A., Ene, E., 2012. FRAGSTATS v4: spatial pattern analysis program for categorical and continuous maps. Computer software program produced by the authors at the University of Massachusetts, Amherst. http://www.umass.edu/landeco/research/fragstats/fragstats.html, 15.
McNab, W.H., Greenberg, C.H., Berg, E.C., 2004. Landscape distribution and characteristics of large hurricane-related canopy gaps in a southern Appalachian watershed. For. Ecol. Manage. 196 (2–3), 435–447.
Meigs, G.W., Keeton, W.S., 2018. Intermediate-severity wind disturbance in mature temperate forests: legacy structure, carbon storage, and stand dynamics. Ecol. Appl. 28 (3), 798–815.
Muller, R.N., Liu, Y., 1991. Coarse woody debris in an old-growth deciduous forest on the Cumberland Plateau, southeastern Kentucky. Can. J. For. Res. 21 (11), 1567–1572.
Nagel, T.A., Svoboda, M., 2008. Gap disturbance regime in an old-growth Fagus-Abies forest in the Dinaric Mountains, Bosnia-Herzegovina. Can. J. Forest Res. 38 (11), 2728–2737.
Nagel, T.A., Mikac, S., Dolinar, M., Klopcic, M., Keren, S., Svoboda, M., Diaci, J., Boncina, A., Paulic, V., 2017. The natural disturbance regime in forests of the Dinaric Mountains: A synthesis of evidence. For. Ecol. Manage. 388, 29–42.
Nagel, T.A., Firm, D., Rozman, A., 2021. Intermediate disturbances are a key driver of long-term tree demography across old-growth temperate forests. Ecol. Evol. 11 (23), 16862–16873.
USDA NRCS, 2022. Web soil survey. Available online at http://websoilsurvey.sc.egov.usda.gov/; last accessed 3 February 2022.
National Oceanic and Atmospheric Administration (NOAA), 2022. Storm events database—event details. National Centers for Environmental Information. Available online at https://www.ncdc.noaa.gov/stormevents/; last accessed 13 January, 2022.
National Oceanic and Atmospheric Administration (NOAA), 2022. Solar position calculator. Available online at https://gml.noaa.gov/grad/solcalc/azel.html; last assessed 20 May 2022.
Oliver, C.D., Larson, B.C., 1996. Forest Stand Dynamics. John Wiley and Sons, New York.
Oswalt, C.M., Kush, J., Barlow, R.J., Gilbert, J.C., 2012. Spatial and temporal trends of the shortleaf pine resource in the eastern United States. In: Proc. of the Shortleaf pine conference: East meets West (No. 11, pp. 33-37). Spec. Rep.
Paluch, J., Jastrzębski, R., 2022. Does natural stand dynamics generate an aggregated pattern of canopy openness? A case study in Abies-Picea-Fagus old-growth forests. For. Ecol. Manage. 507, 119980.
Panayotov, M., Kulakowski, D., Dos Santos, L.L., Bebi, P., 2011. Wind disturbances shape old Norway spruce-dominated forest in Bulgaria. For. Ecol. Manage. 262 (3), 470–481.
Parker, R.P., Hart, J.L., 2014. Patterns of riparian and in-stream large woody debris across a chronosequence of southern Appalachian hardwood stands. Nat. Areas J. 34 (1), 65–78.
Peterson, C.J., 2000. Catastrophic wind damage to North American forests and the potential impact of climate change. Sci. Total Environ. 262 (3), 287–311.
Peterson, C.J., 2007. Consistent influence of tree diameter and species on damage in nine eastern North America tornado blowdowns. For. Ecol. Manage. 250 (1–2), 96–108.
Peterson, C.J., 2019. Damage diversity as a metric of structural complexity after forest wind disturbance. Forests 10 (2), 85.
Peterson, C.J., Cannon, J.B., 2021. Modelling Wind Damage to Southeastern US Trees: Effects of Wind Profile, Gaps, Neighborhood Interactions, and Wind Direction. Front. Forests Global Change.
Peterson, C.J., Cannon, J.B., Godfrey, C.M., 2016. First steps toward defining the wind disturbance regime in central hardwoods forests. In: Natural Disturbances and Historic Range of Variation. Springer, Cham, pp. 89–122.
Pommerening, A., Stoyan, D., 2006. Edge-correction needs in estimating indices of spatial forest structure. Can. J. For. Res. 36 (7), 1723–1739.
Poorter, L., Jans, L., Bongers, F., Van Rompaey, R.S., 1994. Spatial distribution of gaps along three catenas in the moist forest of Tai National Park, Ivory Coast. J. Trop. Ecol. 10 (3), 385–398.
PRISM Climate Group, 2022. Availabel online: www.prism.oregonstate.edu/explorer. Last accessed 24 February 2022.
Rebertus, A.J., Meier, A.J., 2001. Blowdown dynamics in oak-hickory forests of the Missouri Ozarks. J. Torrey Bot. Soc. 128 (4), 362.
Richards, J.D., Hart, J.L., 2011. Canopy gap dynamics and development patterns in secondary Quercus stands on the Cumberland Plateau, Alabama, USA. For. Ecol. Manage. 262 (12), 2229–2239.
Runkle, J.R., 1985. Disturbance regimes in temperate forests. In: Pickett, S.T.A., White, P.S. (Eds.), The Ecology of Natural Disturbance and Patch Dynamics. Academic Press, New York, pp. 17–33.
Rutledge, B.T., Cannon, J.B., McIntyre, R.K., Holland, A.M., Jack, S.B., 2021. Tree, stand, and landscape factors contributing to hurricane damage in a coastal plain forest: Post-hurricane assessment in a longleaf pine landscape. For. Ecol. Manage. 481, 118724.
Salas-Eljatib, C., Weiskittel, A.R., 2020. On studying the patterns of individual-based tree mortality in natural forests: A modelling analysis. For. Ecol. Manage. 475, 118369.
Sefidi, K., Mohadjer, M.R.M., Mosandl, R., Copenheaver, C.A., 2011. Canopy gaps and regeneration in old-growth Oriental beech (Fagus orientalis Lipsky) stands, northern Iran. For. Ecol. Manage. 262 (6), 1094–1099.
Seidl, R., Thom, D., Kautz, M., Martin-Benito, D., Peltoniemi, M., Vacchiano, G., Wild, J., Ascoli, D., Petr, M., Honkaniemi, J., Lexer, M.J., Trotsiuk, V., Mairota, P., Svoboda, M., Fabrika, M., Nagel, T.A., Reyer, C.P.O., 2017. Forest disturbances under climate change. Nat. Clim. Change 7 (6), 395–402.
Seymour, R.S., White, A.S., Philip, G.D., 2002. Natural disturbance regimes in northeastern North America—evaluating silvicultural systems using natural scales and frequencies. For. Ecol. Manage. 155 (1–3), 357–367.
Shearman, T.M., Varner, J.M., Hood, S.M., Cansler, C.A., Hiers, J.K., 2019. Modelling post-fire tree mortality: Can random forest improve discrimination of imbalanced data? Ecol. Model. 414, 108855.

Smalley, G.W., 1986. Classification and evaluation of forest sites on the northern Cumberland Plateau. USDA, Forest Service, Southern Research Experiment Station (General Technical Report SO-60).
Solano, F., Modica, G., Praticò, S., Box, O.F., Piovesan, G., 2022. Unveiling the complex canopy spatial structure of a Mediterranean old-growth beech (Fagus sylvatica L.) forest from UAV observations. Ecol. Ind. 138, 108807.
Stambaugh, M.C., Marschall, J.M., Abadir, E.R., 2020. Revealing historical fire regimes of the Cumberland Plateau, USA, through remnant fire-scarred shortleaf pines (Pinus echinata Mill.). Fire Ecol. 16 (1), 1–15.
Stokes, M.A., Smiley, T.L., 1996. An Introduction to Tree-ring Dating. University of Arizona Press, Tucson.
Stoyan, D., Stoyan, H., 1996. Estimating pair correlation functions of planar cluster processes. Biometrical J. 38 (3), 259–271.
Stueve, K.M., Perry, C.H.(., Nelson, M.D., Healey, S.P., Hill, A.D., Moisen, G.G., Cohen, W.B., Gormanson, D.D., Huang, C., 2011. Ecological importance of intermediate windstorms rivals large, infrequent disturbances in the northern Great Lakes. Ecosphere 2 (1), art2.
Thornthwaite, C.W., 1948. An approach toward rational classification of climate. Geogr. Rev. 38, 55–94.
Trammell, B.W., Hart, J.L., Schweitzer, C.J., Dey, D.C., Steinberg, M.K., 2017. Effects of intermediate-severity disturbance on composition and structure in mixed Pinus-hardwood stands. For. Ecol. Manage. 400, 110–122.
Tzotsos, A., Argialas, D., 2008. Support vector machine classification for object-based image analysis. In: Blaschke, T., Lang, S., Hay, G.J. (Eds.), Lecture Notes in Geoinformation and CartographyObject-Based Image Analysis. Springer Berlin Heidelberg, Berlin, Heidelberg, pp. 663–677.
Van der Meer, P.J., Bongers, F., 1996. Formation and closure of canopy gaps in the rain forest at Nouragues, French Guiana. Vegetatio 126 (2), 167–179.
Vander Yacht, A.L., Keyser, P.D., Harper, C.A., Buckley, D.S., Saxton, A.M., 2017. Restoration of oak woodlands and savannas in Tennessee using canopy-disturbance, fire-season, and herbicides. For. Ecol. Manage. 406, 351–360.
Vexcel Imaging (2022). https://www.vexcel-imaging.com/. Accessed 21 December 2021.
Vickers, L.A., Knapp, B.O., Kabrick, J.M., Kenefic, L.S., D'Amato, A.W., Kern, C.C., MacLean, D.A., Raymond, P., Clark, K.L., Dey, D.C., Rogers, N.S., 2021. Contemporary status, distribution, and trends of mixedwoods in the northern United States. Can. J. For. Res. 51 (7), 881–896.
Villalba, R., Veblen, T.T., 1997. Improving estimates of total tree ages based on increment core samples. Ecoscience 4 (4), 534–542.
Waldron, K., Ruel, J.C., Gauthier, S., 2013. The effects of site characteristics on the landscape-level windthrow regime in the North Shore region of Quebec, Canada. Forestry 86 (2), 159–171.
Wang, H., Yang, F., Luo, Z., 2016. An experimental study of the intrinsic stability of random forest variable importance measures. BMC Bioinf. 17 (1), 1–18.
White, S.D., Hart, J.L., Schweitzer, C.J., Dey, D.C., 2015. Altered structural development and accelerated succession from intermediate-scale wind disturbance in Quercus stands on the Cumberland Plateau, USA. For. Ecol. Manage. 336, 52–64.
White, P.S., Jentsch, A., 2001. The search for generality in studies of disturbance and ecosystem dynamics. Progr. Botany 399–450.
Wiegand, T., Moloney, K.A., 2014. Handbook of spatial point-pattern analysis in ecology. CRC Press.
Woodall, C.W., Heath, L.S., Domke, G.M., Nichols, M.C., 2011. Methods and equations for estimating aboveground volume, biomass, and carbon for trees in the US forest inventory, 2010. Gen. Tech. Rep. NRS-88. Newtown Square, PA: US Department of Agriculture, Forest Service, Northern Research Station. 30 p., 88, 1-30.
Woodall, C.W., Graham, J.M., 2004. A technique for conducting point pattern analysis of cluster plot stem-maps. For. Ecol. Manage. 198 (1–3), 31–37.
Woods, K.D., 2004. Intermediate disturbance in a late-successional hemlock-northern hardwood forest. J. Ecol. 464–476.
Yamamoto, S.I., 1995. Gap characteristics and gap regeneration in subalpine old-growth coniferous forests, central Japan. Ecol. Res. 10 (1), 31–39.